AD-A119 410 STANFORD UNIV CA DEPT OF STATISTICS F/G 12/1
SEQUENTIAL STOCHASTIC CONSTRUCTION OF RANDOM POLYGONS.(U)
JUN 82 E I GEORGE N00014-76-C-0475
UNCLASSIFIED TR-320 NL

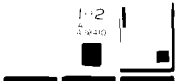

SEQUENTIAL STOCHASTIC CONSTRUCTION OF RANDOM POLYGONS

By

Edward Ian George

TECHNICAL REPORT NO. 320

JUNE 10, 1982

Prepared Under Contract
N00014-76-C-0475 (NR-042-267)
For the Office of Naval Research

Herbert Solomon, Project Director

DEPARTMENT OF STATISTICS
STANFORD UNIVERSITY
STANFORD, CALIFORNIA

TABLE OF CONTENTS

Page

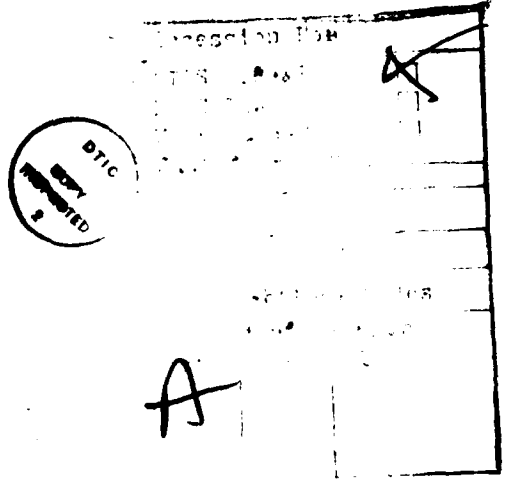

LIST OF TABLES

INTRODUCTION

0.1. Motivation.

Research on the idea of random polygons formed by random lines in the plane, the subject of the present thesis, was first motivated in the literature by the physicist Goudsmit (1945). Concerned with the positioning of particle tracks in early cloud-chamber experiments, Goudsmit wanted to know if the distribution of these tracks was random. He considered the general model of "a plane covered with straight lines distributed at random in position and direction". Observing that these lines subdivide or tessellate the plane into polygons, see Figure 0.1, he posed the problem of finding the probability distribution of the areas of these fragments. Presumably, if he could measure the areas of the polygons formed between the tracks, knowledge of these distributions would pave the way for statistical investigations of the actual positioning process.

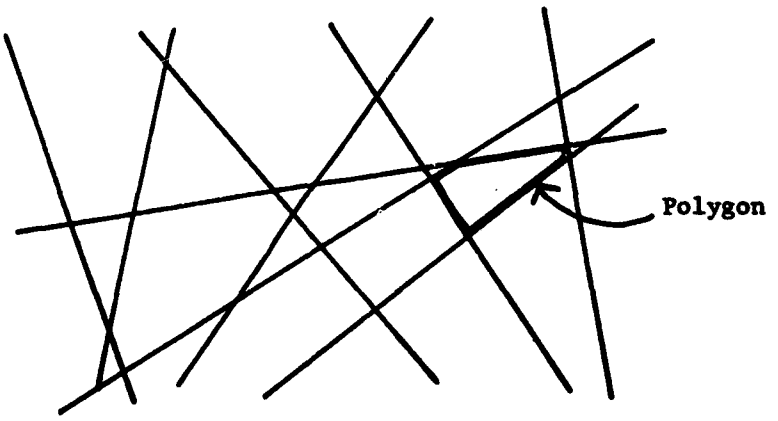

Figure 0.1.

Rather than attack the general problem, Goudsmit considered three easier problems. He first solves the problem for the simplified case where lines are limited to two perpendicular directions. He next considers the idealized problem on a sphere with random great circles replacing lines, "in order to avoid difficulties with infinity". By counting arguments he obtains the mean area, and observes that as the diameter of the sphere is increased while the density of lines is held constant, the tessellation characteristics approach those in the planar case. Finally, Goudsmit finds the mean square area for polygons with a clever ad hoc technique, reminiscent of the method of Crofton. For a comprehensive account of Goudsmit's work, including extensions and generalizations, see Solomon (1978).

0.2. Recent Research

By far the most significant contributor to research on this problem has been R. E. Miles. Miles (1964) reports on the findings of his (unpublished) Ph.D. dissertation in which he lists the essential properties of the models on which the present work is based. Modelling random lines in the plane by homogeneous Poisson fields of lines (see Section 1.1) [1], Miles investigates the distribution of other polygon characteristics besides A, the area, such as N, the number of sides, S, the perimeter, and D, the in-circle diameter [2]. Though he presents (without proof) many impressive partial results and alludes to others, he concludes by stating that

> "The central open questions are clearly the determination in the isotropic case of the distributions of N, S, and (especially) A. ... Failing exact methods, a Monte Carlo study would seem to offer an excellent way of approximating this particular distribution and others."

Miles (1971) generalizes the problem to higher dimensions and establishes the ergodic theory for future work. Miles (1973) derives the explicit form of certain ergodic distributions, establishes relationships between different polygon populations in the tessellation, and suggests stochastic constructions for polygons similar in spirit to the one developed here [3]. Miles (1974) develops some sampling theory pertinent to methods used in the Monte Carlo study by Crain and Miles (1976).

Concise summaries and extensive bibliographies of recent work on generalizations of this problem and related problems can be found in Moran (1966, 1969), Little (1974), and Baddeley (1977). General random line processes are discussed at length in Harding and Kendall (1974).

0.3. The Present Work

This dissertation develops a different point of view as to the genesis of aggregates of polygons formed by Poisson fields of random lines. When seen as resulting from a tessellation, the polygon aggregate is a secondary formation in the sense that it is not determined until the entire field of lines has been realized. However, the realization of each polygon is a random event in its own right. A sequential stochastic point process, called the curling process, is constructed. It is distinct from the Poisson line process and generates polygons one at a time. In effect, this process can select an independent and identically distributed sample of polygons from the polygon aggregate in a Poisson field of lines.

As well as lending insight into the dynamics of polygon formation, the curling process is a fruitful tool for the investigation of the distributions of polygon characteristics. In particular, it yields a high speed computer simulation technique for Monte Carlo studies of these characteristics. Furthermore, the curling process is specified in the general translation invariant context. Hence, it can be used to explore anisotropic alternatives in addition to the isotropic (rotationally invariant) case.

The outline of this work is as follows. Chapter 1 defines the Poisson line processes that are used to model random lines in the plane. Basic results which are required to develop the curling process are proved there. Chapter 2 defines the curling process and develops its

distributional characteristics. Chapter 3 contains derivations of the polygon distributions from the curling process and explores methods for deriving distributions of polygon characteristics. It also contains definitions of useful families of anisotropic alternatives to isotropy. Chapter 4 contains a Monte Carlo study of the distributions of polygon characteristics over a wide range of Poisson line distributions. Therein are established some theorems which enable the use of a high speed version of the curling process for simulation.

CHAPTER 1

POISSON LINE PROCESSES

1.1. Poisson Fields of lines.

We parametrize each line in the plane by (p,θ) where $p \in (-\infty,\infty)$ is the (signed) perpendicular distance of the line from the origin O, and $\theta \in [0,\pi)$ [4] is the northeast angle that this line makes with the horizontal, see Figure 1.1.

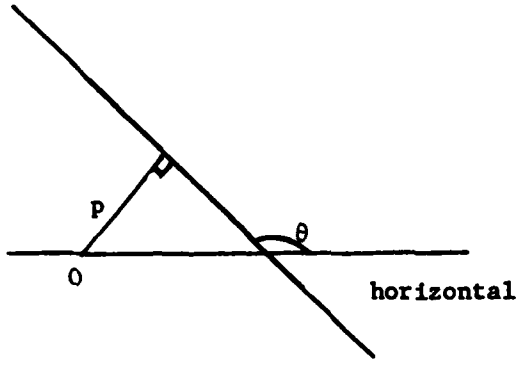

Figure 1.1.

A set of lines

$$\mathcal{L} = \{(p_i,\theta_i) , \quad i = 0,\pm1,\pm2,\ldots\} \tag{1.1}$$

is said to be a <u>Poisson field of lines</u> if

(1.2) i) $-\infty < \cdots < p_{-1} < p_0 < p_1 < p_2 < \cdots < \infty$ is a realization of a linear Poisson process of constant intensity $\tau > 0$. (See the appendix) for definitions of the Poisson process).

(1.3) ii) $\{\theta_i\}$ are realizations of independent and identically distributed random variables with arbitrary distribution $G(\theta)$, $\theta \in [0,\pi)$. Furthermore the angles $\{\theta_i\}$ are independent of the distances $\{P_i\}$.

A Poisson line process is that random process whose realization is a Poisson field of lines.

The (p,θ) parametrization makes clear the bijective correspondence between lines in $\mathbb{R}^2$ and the cylinder

$$C = \{(p,\theta): \; p \in (-\infty,\infty) \; , \; \theta \in [0,\pi)\} \; . \tag{1.4}$$

Equivalently we can define a Poisson line process to be a two-dimensional Poisson point process N on C. More precisely, N is a non-negative integer-valued random Borel measure on C [5] which satisfies for disjoint Borel $A_1,\ldots,A_k$ on C and some $\tau > 0$,

$$\Pr\left(\bigcap_{i=1}^{k} (N(A_i) = n_i)\right) = \prod_{i=1}^{k} \left\{ e^{-\tau m(A_i)} (\tau m(A_i))^{n_i}/n_i! \right\} \tag{1.5}$$

where

$$m(A) = \int_A dp \; dG(\theta) \; . \tag{1.6}$$

[6]

(For consistency with (1.3) we choose G suitably normalized to be a probability distribution.)

It should be pointed out that there are several equivalent ways of generating a Poisson field of lines. We shall however, regard the process N on C defined by (1.5) and (1.6) as our starting point and use it to prove many of the basic results in Section 1.2.

We now proceed to show how $m(A)$ in (1.6) arises solely from invariance considerations. Let J^* be the group of translations of R^2. Let J be the group of motions on C induced by J^*. For the following results it will be convenient to consider the angle ϕ that the perpendicular from O to a line makes with the origin. See Figure 1.2.

Figure 1.2.

In terms of θ we have

$$\phi = \begin{cases} \theta + \frac{\pi}{2} & \text{for } \theta \in [0, \frac{\pi}{2}) \\ \theta - \frac{\pi}{2} & \text{for } \theta \in [\frac{\pi}{2}, \pi) \end{cases} . \tag{1.7}$$

The relationship between (p,θ) and the cartesian coordinates (x,y) of its points in R^2 is then

$$x \cos \phi + y \sin \phi - p = 0 . \tag{1.8}$$

J^* is clearly generated by motions of the form

$$T^*_{(x^*,y^*)} : (x,y) \mapsto (x+x^*,\ y+y^*) \ , \quad \text{for} \quad (x^*,y^*) \in \mathbb{R}^2 \ .$$

This motion sends (1.8) into

$$x \cos \phi + y \sin \phi - (p - x^* \cos \phi - y^* \sin \phi) = 0 \ .$$

Thus J is generated by motions of the form

$$(1.9) \quad T_{(x^*,y^*)} : (p,\theta) \mapsto (p - x^* \cos \phi - y^* \sin \phi,\ \theta), \ \text{for} \ (x^*,y^*) \in \mathbb{R}^2 \ ,$$

with ϕ related to θ by (1.7). It is interesting to note that (1.9) is a shear and not a translation of C. In fact, J contains no translations.

Theorem 1.1.1. Every positive Borel measure m on C invariant under J is expressible, up to positive factors, in the form (1.6).

Proof. We shall prove the theorem for the case where m is expressible in the form

$$(1.10) \qquad m(A) = \int_A f(p,\theta)\, dp\, d\theta$$

for all Borel A on C.

If m is invariant under J we have from (1.9)

(1.11) $$m(A) = m(T_{(x^*,y^*)} A) \qquad \forall\, (x^*,y^*) \in \mathbb{R}^2$$

where

(1.12) $$T_{(x^*,y^*)} A = \{(p,\theta): T^{-1}_{(x^*,y^*)}(p,\theta) \in A\} .$$

But (1.10), (1.11) and (1.12) imply that $\forall\, (x^*,y^*) \in \mathbb{R}^2$

$$\int_A f(p,\theta)\, dp\, d\theta = \int_{T_{(x^*,y^*)} A} f(p,\theta)\, dp\, d\theta$$

$$= \int_A f(p - x^* \cos\phi - y^* \sin\phi\, ,\theta)\, dp\, d\theta$$

$$\Rightarrow \quad f(p,\theta) = f(p - x^* \cos\phi - y^* \sin\phi,\ \theta) \qquad \forall (x^*,y^*) \in \mathbb{R}^2 .$$

Hence, $f(p,\theta) = g(\theta)$ say, is a function of θ only and

$$m(A) = \int_A g(\theta)\, dp\, d\theta = \int_A dp\, dG(\theta) . \quad \|$$

Theorem 1.1.1 illustrates how (p,θ) (or (p,ϕ)) is a natural parametrization of lines in the plane with respect to translation invariant measures.

We say that a line process is <u>homogeneous</u> if the distribution of the process is translation invariant, i.e. the distribution of the process is invariant under the actions of J^*.

Theorem 1.1.2. The Poisson line process is homogeneous iff (1.6) holds for the characterizing point process N defined by (1.5).

Proof. If the Poisson line process is homogeneous, then N is invariant on C under $\mathfrak{J}$. But then so is $EN(A) = \tau m(A)$ invariant under $\mathfrak{J}$ for all A on C. It follows from Theorem 1.1.1 that for suitably chosen $\tau > 0$, (1.6) holds.

The reverse implication follows directly from the demonstrated invariance of $m(A) = \int_A dp\, dG(\theta)$ derived in Theorem 1.1.1. ||

The special case of homogeneity of most interest is that where the group of motions is enlarged to include rotations. We denote this enlarged group by $\mathfrak{M}^*$, and the group of induced motions on C by $\mathfrak{M}$. Davidson (1974) showed that $\mathfrak{M}$ on C is generated by motions of the form

$$R_\omega: (p,\theta) \longmapsto (p,\theta+\omega) , \qquad \text{for } \omega \in [0,\pi)$$

and

$$S_s: (p,\theta) \longmapsto (p+\cos\phi,\theta) , \text{ for } s \in \mathbb{R}$$

analogous to (1.9).

We also have the well known analogue of Theorem 1.1.1.

Theorem 1.1.3. (Crofton (1885), Santalo (1953)). There is, up to positive factors, a unique positive Borel measure ρ on C invariant under $\mathfrak{M}$, and this measure (which we shall denote by m_I), is of the form

(1.13) $\quad m_I(A) = \frac{1}{\pi} \int_A dp\, d\theta \quad$ for all Borel A on C .

(The factor $\frac{1}{\pi}$ appears in (1.13) for consistency with the definition of G in (1.3) as a probability distribution.)

We say that a line process is homogeneous and isotropic if the process is translation and rotation invariant, i.e. the distribution of the process is invariant under the actions of $\mathfrak{M}^*$. We have the following analogue of Theorem 1.1.2 which is proved with the same argument replacing Theorem 1.1.1 by Theorem 1.1.3.

Theorem 1.1.4. The Poisson line process is homogeneous and isotropic iff (1.13) holds for the characterizing point process N defined by (1.5).

Throughout the sequel we shall only concern ourselves with homogeneous Poisson line processes. We call those line processes which are not isotropic, anisotropic. By a slight abuse of terminology, we will refer to isotropic and anisotropic Poisson fields of lines when the line process generating them has those properties.

1.2. The Basic Theorems.

In this section we derive the probability distributions of certain types of events in a Poisson field of lines. These are known results which can be derived in a variety of ways. We use the following idea. By expressing each event as the realization of points in a particular set A on C our results follow directly from (1.5) once we have found $m(A)$ or $m_I(A)$.

We shall find it convenient to allow θ, the orientation angle, to be in the range $[-\pi,2\pi]$. It is to be understood that such a θ refers to a line with orientation $\theta \bmod \pi$. We generalize the distribution $G(\theta)$ by

$$dG(\theta) = dG(\theta \bmod \pi) \ . \tag{1.14}$$

The following theorems concern intersections of a Poisson field with a line. Let ℓ_0 be an arbitrary line in $\mathbb{R}^2$ with orientation $\theta_0(\varepsilon[0,\pi))$. For definiteness, we define the angle of intersection of another line with ℓ_0 by $\omega = \theta-\theta_0$, where lines are now parametrized by (p,θ) with $\theta_0 \le \theta \le \theta_0 + \pi$ understood in the sense above.

Fix a segment C of length c on ℓ_0 and define

$$A_C(\omega) = \{(p,\theta): \text{the line } (p,\theta) \text{ intersects } C \text{ and } 0 < (\theta-\theta_0) \le \omega\} \ . \tag{1.15}$$

Theorem 1.2.1.

$$m(A_C(\omega)) = c \int_{\theta_0}^{\theta_0+\omega} \sin(\theta-\theta_0)\, dG(\theta) \tag{1.16}$$

Proof. By translation invariance, we may locate C with the southermost end at the origin, 0. Consider an arbitrary line (p,θ) intersecting C at length s from 0. See Figure 1.3.

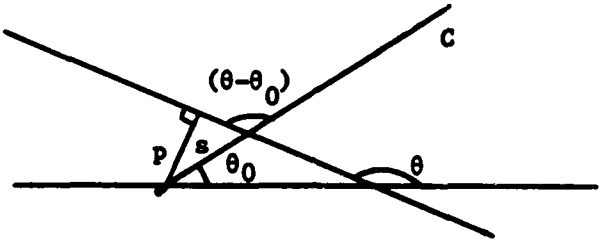

Figure 1.3.

Reparametrizing (p,θ) by (s,θ), we have

$$p = s \sin(\theta-\theta_0) \Rightarrow dp\, dG(\theta) = \sin(\theta-\theta_0) ds\, dG(\theta) .$$

Hence,

$$\begin{aligned} m(A_C(\omega)) &= \int_{A_C(\omega)} dp\, dG(\theta) \\ &= \int_{\theta_0}^{\theta_0+\omega} \int_0^c \sin(\theta-\theta_0) ds\, dG(\theta) \\ &= c \int_{\theta_0}^{\theta_0+\omega} \sin(\theta-\theta_0)\, dG(\theta) . \end{aligned}$$ ||

In the isotropic case $dG(\theta) \equiv \frac{1}{\pi}\, d\theta$, and

$$(1.17) \qquad m_I(A_C(\omega)) = \frac{c}{\pi} \int_{\theta_0}^{\theta_0+\omega} \sin(\theta-\theta_0)d\theta = \frac{c}{\pi} \int_0^{\omega} \sin\theta\, d\theta \quad .$$

The above results are the building blocks of the following theorems.

Theorem 1.2.2. Points of intersection of $\mathcal{L}$ with ℓ_0 are realizations of a linear Poisson process of constant intensity $\tau\lambda(\theta_0)$ where

$$(1.18) \qquad \lambda(\theta_0) = \int_{\theta_0}^{\theta_0+\pi} \sin(\theta-\theta_0)\, dG(\theta) = \int_0^{\pi} |\sin(\theta-\theta_0)|dG(\theta) \quad .$$

The result holds conditionally for $\ell_0 \in \mathcal{L}$.

Proof. It follows from Theorem 1.2.1 that for any set of intervals $C_1,\ldots,C_n$ of lengths $c_1,\ldots,c_n$,

$$(1.19) \qquad m(A_{C_i}(\pi)) = \lambda(\theta_0)c_i$$

(1.5) implies that intersections of $\mathcal{L}$ with C_i have a Poisson distribution with mean $\tau\lambda(\theta_0)c_i$. Furthermore, if the C_i's are disjoint, intersections with $C_1,\ldots,C_n$ are mutually independent. This is sufficient to characterize the linear Poisson process along ℓ_0 of (constant) intensity $\tau\lambda(\theta_0)$ (see characterization (A.1) in the appendix).

Finally, the result holds conditionally on $\ell_0 \in \mathcal{L}$ because ℓ_0 was arbitrary. ||

For isotropic $\mathcal{L}$, Theorem 1.2.2 holds with

$$\lambda(\theta_0) \equiv \frac{2}{\pi}, \tag{1.20}$$

since from (1.17)

$$m_I(A_{C_i}(\pi)) = \frac{c_i}{\pi} \int_0^{\pi} \sin\theta \, d\theta = \frac{2c_i}{\pi}. \tag{1.21}$$

Theorem 1.2.3. In Theorem 1.2.2, the angles associated with points of intersection are independent and identically distributed with common distribution

$$H^{\theta_0}(\omega) = (\lambda(\theta_0))^{-1} \int_{\theta_0}^{\theta_0+\omega} \sin(\theta-\theta_0) \, dG(\theta) \tag{1.22}$$

for $\omega \in (0,\pi)$. These angles are also independent of the p_i's associated with the intersecting lines.

Proof. Consider again the interval C on ℓ_0.

Conditional on n intersections with C, i.e. $N(A_C(\pi)) = n$, let $\{(p_i,\theta_i)\}_{i=1}^n$ denote the (reindexed) parametrizations of the intersecting lines.

It follows from (1.5) that [7]

$$\{(P_i,\Theta_i) \,|\, N(A_C(\pi)) = n\}_{i=1}^n$$

are independent and identically distributed with common density

$$(m(A_C(\pi)))^{-1} \, dp \, dG(\theta) \quad \text{on} \quad (p,\theta) \in A_C(\pi) \, . \; [8]$$

Thus, since C is arbitrary,

$$H^{\theta_0}(\omega) = P\{(P,\Theta) \in A_C(\omega) \mid N(A_C(\omega)) > 0\}$$

$$= (m(A_C(\pi)))^{-1} \int_{A_C(\omega)} dp\, dG(\theta)$$

$$= \frac{m(A_C(\omega))}{m(A_C(\pi))}$$

$$= \frac{c \int_{\theta_0}^{\theta_0+\omega} \sin(\theta-\theta_0)\, dG(\theta)}{c\, \lambda(\theta_0)}$$

by (1.16) and (1.18).

Independence of angles among disjoint intervals is immediate from (1.5). The independence of the angles from the p_i's is immediate from the absence of p_i in (1.22). ||

Results in the isotropic case are again much simpler where Theorem 1.2.3 holds with

$$(1.23) \qquad H^{\theta_0}(\omega) = \left(\frac{2}{\pi}\right)^{-1} \frac{1}{\pi} \int_{\theta_0}^{\theta_0+\omega} \sin(\theta-\theta_0)d\theta = \frac{1}{2} \int_0^{\omega} \sin\theta\, d\theta$$

independent of θ_0 as we should expect.

It follows immediately from (1.22) that the density of the angles of lines intersecting ℓ_0 is

$$(1.24) \qquad dF_{\theta|\theta_0}(\theta) = (\lambda(\theta_0))^{-1} |\sin(\theta-\theta_0)| dG(\theta) .$$

Using the convention (1.14), the support of (1.23) can be any interval of length π.

In the isotropic case (1.23) is just

$$dF_\theta(\theta) = \frac{1}{2} \sin\theta \, d\theta \ . \tag{1.25}$$

Theorem 1.2.4. Consider T an arbitrary triangle with sides T_1, T_2, T_3 of lengths t_1, t_2, t_3 and orientations $\theta_1, \theta_2, \theta_3$ respectively. Then the number of intersections of $\mathcal{L}$ with T has a Poisson distribution with mean

$$\frac{\tau}{2} \left(t_1\lambda(\theta_1) + t_2\lambda(\theta_2) + t_3\lambda(\theta_3)\right) \ . \tag{1.26}$$

The number of intersections of $\mathcal{L}$ with T which do not intersect side T_3 has a Poisson distribution with mean

$$\frac{\tau}{2} \left(t_1\lambda(\theta_1) + t_2\lambda(\theta_2) - t_3\lambda(\theta_3)\right) \ . \tag{1.27}$$

Proof. Let

$$B = \{(p,\theta): (p,\theta) \text{ intersects } T\}$$

and

$$B_- = \{(p,\theta): (p,\theta) \text{ intersects } T \text{ but not } T_3\} \ .$$

Since each line intersecting T intersects two sides, we have in the notation of (1.15)

$$2m(B) = \sum_{i=1}^{3} m(A_{B_i}(\pi))$$

and

$$2m(B_{-}) = m(A_{B_1}(\pi)) + m(A_{B_2}(\pi)) - m(A_{B_3}(\pi)) .$$

But as in (1.19),

$$m(A_{T_i}(\omega)) = t_i\lambda(\theta_i) .$$

Hence the desired assertions follow from (1.5). ||

We remark that by (1.20), Theorem 1.2.4 holds in the isotropic case with (1.26) replaced by

$$\frac{\tau}{\pi}(t_1 + t_2 + t_3) \tag{1.28}$$

and (1.27) replaced by

$$\frac{\tau}{\pi}(t_1 + t_2 - t_3) . \tag{1.29}$$

The next result involves the distributions of angles of intersections of members of $\mathcal{L}$. As opposed to our use of integral geometry to evaluate the measure of sets above, we find a conditional probability argument simpler now.

Theorem 1.2.5. Angles of intersection between members of $\mathcal{L}$ have the marginal distribution

$$H(\omega) = \lambda^{-1} \iint_{\substack{0<|\theta_1-\theta_0|\le\omega \\ \theta_1\in[0,\pi) \\ \theta_0\in[0,\pi)}} |\sin(\theta_1-\theta_0)| \, dG(\theta_1) \, dG(\theta_0) \tag{1.30}$$

where

$$\lambda = \int_0^{\pi} \lambda(\theta_0)\, dG(\theta_0) \tag{1.31}$$

and $\omega \in (0,\pi)$.

Proof. By unconditioning (i.e. integrating over the range of θ_0) the result of Theorem 1.2.3, we obtain

$$H(\omega) \propto \iint_{0 \le \theta_0 < \theta_1 < \theta_0 + \pi \le 2\pi} \sin(\theta_1 - \theta_0)\, dG(\theta_1)\, dG(\theta_0)$$

which is identical with (1.30) using (1.14). λ is then the correct normalizing constant. ||

Notice that in the isotropic case, since (1.23) does not depend on θ_0, we have immediately that

$$H(\omega) = \frac{1}{2} \int_0^{\omega} \sin\theta\, d\theta \quad \text{for} \quad \omega \in (0,\pi) . \tag{1.32}$$

It follows immediately from (1.22) that the joint density of the angles of lines at intersection points is

$$dH(\theta_0,\theta_1) = \lambda^{-1} |\sin(\theta_1 - \theta_0)| dG(\theta_1) dG(\theta_0) . \tag{1.33}$$

Using (1.14), the support of (1.33) is the direct product of any two intervals, each of length π.

In the isotropic case (1.33) is just

$$dH(\theta_0,\theta_1) = \frac{1}{2\pi}\,|\sin(\theta_1-\theta_0)|\,d\theta_1 d\theta_0 \,. \tag{1.34}$$

The result (1.34) is somewhat counterintuitive since lines in an isotropic field would seem to meet at uniformly distributed angles. (1.34) reflects the fact that angles far from perpendicular are 'shifted' out towards 'infinity'.

CHAPTER 2
THE CURLING PROCESS

Every realization of a Poisson line process subdivides the plane into a set of non-overlapping polygons. Borrowing from the notation of Miles (1973), we denote the aggregate of polygons from a single realization by ρ^*. ρ^* refers to the general case; we use the terms isotropic ρ^* and anisotropic ρ^* to refer to the polygon aggregate in the isotropic and anisotropic cases, respectively. In this chapter we develop a sequential stochastic process, which we shall hereafter call the curling process, capable of generating an independent and identically distributed sample of polygons from the population of polygons equivalent to any ρ^* up to translation. [9] The reduction of members of ρ^* by invariance is an advantage since virtually all of the polygon characteristics of interest are invariant under the groups of motion considered.

2.1. Which Distributions?

As is discussed in the introduction, of substantial interest to research workers in this area, has been the distributional properties of certain characteristics of members of ρ^*, principally N, the number of sides, S, the perimeter, and A, the area. Two questions come to mind as to what is meant by the distribution of characteristics here. Namely, how does one define a distribution for a single realization ρ^*, and is the distribution the same for all ρ^*? The prior work of Miles (1964, 1973) answers these questions. By exploiting the homogeneity of the Poisson line process Miles is able to

demonstrate the existence of ergodic distributions as the limits of empirical distributions of polygons contained in a disc of radius q as $q \to \infty$. These ergodic distributions are the same for all ρ^* (w.p.1). Miles even obtains explicit forms for certain characteristics, though not for the ones mentioned.

The distribution of polygons obtained by the curling process turns out to be exactly the ergodic distribution obtained by Miles though we do not base our derivation on ergodic results. All of the probabilistic results in Section 1.2 are based on the population of all realizations of a Poisson line process. The curling process is derived from these results and hence is based on the distribution of of all polygons obtained from all ρ^*'s. We shall depote this super-population by ρ^{**}. However, the eventual agreement with Miles' results shows that our results apply equally well to the population of polygons in a single ρ^*.

2.2. Notation.

Consider an arbitrary N-sided convex polygon. Label by θ_0, the angle that the right side of the southernmost vertex (if there are two choose the one on the left), makes with the horizontal. Starting from this vertex label consecutively, in clockwise direction, the side lengths $Z_1, Z_2, \ldots, Z_N$, and the angles that these sides make with the horizontal $\theta_1, \theta_2, \ldots, \theta_N$. Figure 2.1 is an example of this labeling for $N = 5$.

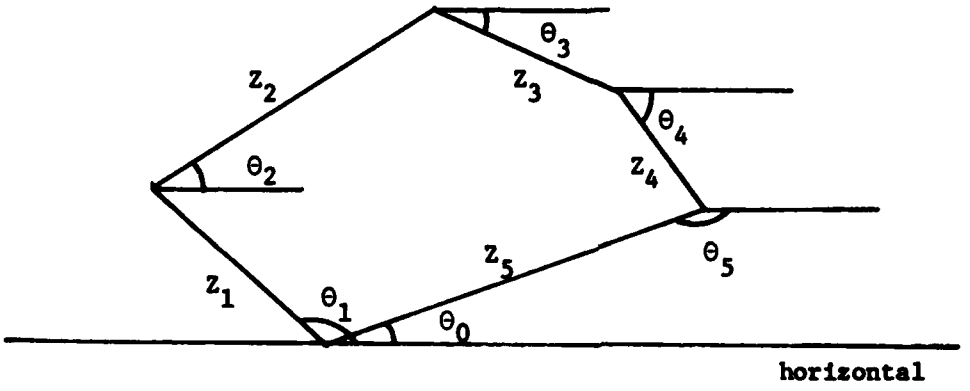

Figure 2.1. The notation for a 5-sided polygon

We denote the lines coinciding with $Z_1, Z_2, \ldots, Z_N$ by $\ell_1, \ell_2, \ldots, \ell_N$ and the vertices corresponding to $\theta_1, \theta_2, \ldots, \theta_N$ by $V_1, V_2, \ldots, V_N$. It will be convenient to define $\ell_0 = \ell_N$. for notational ease let

$$\theta^{(n)} = (\theta_0, \theta_1, Z_1, \theta_2, Z_2, \ldots, Z_{n-1}, \theta_n) \tag{2.1}$$

and

$$z^{(n)} = (\theta^{(n)}, Z_n) \quad . \tag{2.2}$$

Since

$$\theta_N = \theta_0 - \pi \ , \quad \sum_{i=1}^{N} Z_i \sin \theta_i = 0 \ , \quad \sum_{i=1}^{N} Z_i \cos \theta_i = 0 \ . \tag{2.3}$$

N and $\theta^{(N-1)}$ are sufficient to specify any polygon in ρ^{**} up to translation. For isotropic ρ^{**}, we will force $\theta_0 \equiv 0$, in which case N and $\theta^{(N-1)}$ are sufficient to specify a polygon up to translation and rotation.

We denote the perimeter by S where

$$S = \sum_{i=1}^{N} Z_i \ , \tag{2.4}$$

which can be reduced to a function of $\theta^{(N-1)}$ by (2.3).

If we also consider the polygon to be located in the Cartesian plane with the origin located at v_1, we find the Cartesian coordinates of the vertices useful. These may be related to the θ's and Z's by

$$\begin{cases} (X_i, Y_i) = \left(\sum_{j=1}^{i} Z_j \cos \theta_j \ , \ \sum_{j=1}^{i} Z_j \sin \theta_j \right) \\ (X_0, Y_0) = (0,0) \ . \end{cases} \tag{2.5}$$

We denote the area by A. By considering successive areas of triangles

and quadrilaterals formed by consecutive sides over the x-axis we obtain the following convenient expression for A.

$$A = \frac{1}{2} \sum_{i=1}^{N} (X_i - X_{i-1})(Y_i + Y_{i-1}) \,. \tag{2.6}$$

This can be related to the Θ's and Z's by (2.5), and further reduced by (2.3).

In the sequel we shall be treating much of the above notation as representing random variables.

2.3. The Curling Process Conceptually

We now proceed to describe very generally the curling process. Each realization of the curling process is an infinite alternating sequence of angles and side lengths. As will be seen, from each of these realizations we can extract one polygon, so that polygons are a by-product of the curling process just as they are a by-product of the line process. However, although our construction of the curling process is based on the properties of the Poisson line process derived in Section 1.2, it is important to regard the two processes as separate entities.

In Figure 2.2 we heuristically portray the sequential realization of the curling process. (Angle selection is indicated by the dashed lines, and side lengths by the solid lines). The polygon to be extracted from the process is distinguished from the curling process by the bold outline at the end.

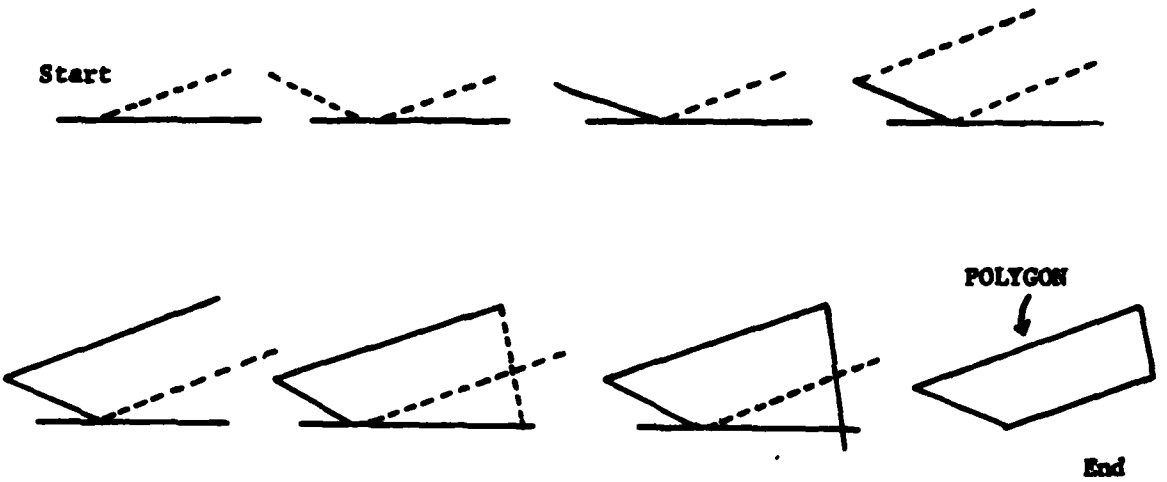

Figure 2.2

As Figure 2.2 demonstrates, the polygon and the curling process coincide initially. Because of this coincidence we use essentially the same notation for each. That is, the curling process is denoted by the same sequence

$$\theta_0,\theta_1,z_1,\theta_2,z_2,\theta_3,z_3,\cdots$$

corresponding to the polygon notation developed in Section 2.2. It should be clear from the context which coordinates we are referring to. However, when ambiguity might arise, or it is necessary to distinguish between the two, we will put '~' over the symbol when expressly referring to the curling processes. For example, given that the polygon to be extracted as N sides, one can conclude from Figure 2.2 that $\tilde{z}_{N-1}$ is the first coordinate of the curling process which might depart from the corresponding coordinate z_{N-1} of the polygon formed. Specifically, we will define N (or more precisely

N-1) as a stopping time so that the first 2N-2 coordinates of the curling process coincide with the first 2N-2 coordinates of the polygon, $\theta^{(N-1)}$. Since the remaining polygon coordinates are determined through (2.3), the polygon distribution is obtained from the distribution of the first 2N-1 coordinates of the curling process.

Just as in Figure 2.2, our development and specification of the curling process will be sequential. This point of view is simpler, clearer, and greatly facilitates Monte Carlo simulation. As the process is highly dependent, we condition on the past at each step using conventional conditional probablity arguments. In particular, we regard the past as a realized sequence pertaining to the selection of a polygon. The joint distribution of the curling process is obtained as the product of the derived conditional probabilities. The stopping time N is determined by the first side length to cross ℓ_0. Thus, the polygon coinciding with the curling process has as its last vertex v_N, the intersection of the curling process with ℓ_0. Though the curling process conceptually continues forever, we will not concern ourselves with its behavior beyond this stopping time.

In the remainder of this chapter we develop the sequential and joint distributional properties of the curling process. The joint distribution yields expressions concerning the distributions of characteristics of members of ρ^{**}, which we explore in Chapter 3. The sequential distributions are the basis of the Monte Carlo simulation studies in Chapter 4. There we derive some results concerning simulation of these sequential distributions which are equivalent yet faster computationally. In this sense the final curling process we use is defined in that chapter.

2.4. The Joint Distribution of θ_0 and θ_1 - Picking a Polygon Randomly.

$\theta^{(1)} = (\theta_0, \theta_1)$ determines the orientation and size of the southernmost angle of a polygon. The following proposition apparently first observed by M. Stone (Miles (1964)), links the distribution of this angle to the distribution of certain intersection angles, and enables us to sample a member of ρ^{**}.

Proposition. In any realization of a line process, there exists a bijective map between the points of intersection of lines and members of the polygon aggregate induced.

Proof. Associate with each polygon, that intersection point corresponding to the vertex which is southernmost. If there are two, choose the one on the left. This choice is unique. Similarly, associate with each intersection point that polygon which lies entirely above it. If there are two, choose the one on the right. This choice is unique. ||

(Note that the choice of south is arbitrary here).

Hence to sample a polygon from ρ^{**}, we need only sample southernmost vertices which, by the proposition, correspond to sampling northernmost angles at intersection points. It follows that the joint distribution of θ_0 and θ_1 can be obtained from (1.32) by a symmetry argument as

$$(2.7) \qquad dF_{\theta_0,\theta_1}(\theta_0,\theta_1) = \frac{2}{\lambda} \sin(\theta_1-\theta_0)\, dG(\theta_1)\, dG(\theta_0)$$

for $0 \leq \theta_0 < \theta_1 \leq \pi$.

As we are interested in specifying the curling process sequentially, we need the marginal distribution of θ_0 which can be computed (in principle) for specific instances of G from

$$(2.8) \qquad dF_{\theta_0}(\theta_0) = \frac{2}{\lambda}\, dG(\theta_0) \cdot \int_{\theta_0}^{\pi} \sin(\theta-\theta_0)\, dG(\theta) ,$$

for $\theta_0 \in [0,\pi)$.

Next, given θ_0, θ_1 is selected from the conditional density

$$(2.9) \qquad dF_{\theta_1|\theta_0}(\theta_1) = \left[\int_{\theta_0}^{\pi} \sin(\theta-\theta_0)\, dG(\theta)\right]^{-1} \cdot \sin(\theta_1-\theta_0)\, dG(\theta_1)$$

for $0 \leq \theta_0 < \theta_1 \leq \pi$.

In the isotropic case, the actual value of θ_0 will be unimportant because of the rotational invariance. In this case we begin the curling process with the angle $(\theta_1-\theta_0)$. The marginal distribution of $\theta = (\theta_1-\theta_0)$ for isotropic P^{**} is derived from (2.7) as ($\lambda = 2\pi$ from (1.34))

$$dF(\theta) = \frac{1}{\pi} \sin\theta\, d\theta \int_0^{(\pi-\theta)} d\theta_0 = \frac{\pi-\theta}{\pi} \sin\theta\, d\theta \quad .$$

Thus, for isotropic P^{**}, without loss of generality we assume $\theta_0 \equiv 0$ and begin the curling process by selecting θ_1 from the density

$$(2.10) \qquad dF_{\theta_1}(\theta_1) = \frac{\pi-\theta_1}{\pi} \sin\theta_1\, d\theta_1$$

for $0 \leq \theta_1 \leq \pi$.

It is interesting to compare this choice of θ_1 with the naive guess $dF_{\theta_1}(\theta_1) = \frac{1}{2} \sin \theta_1 \, d\theta_1$. This is tantamount to choosing an arbitrary vertex in the plane. The sample of polygons so chosen will be weighted by the number of vertices. This particular aggregate of polygons are the N-polygons described by Miles (1973).

2.5. The Conditional Distribution for General $(\theta_n | z^{(n-1)})$.

From (1.24) we know that the conditional density of $(\theta_n | z^{(n-1)})$ is proportional to

$$dF_{\theta_n | z^{(n-1)}}(\theta_n) \propto |\sin(\theta_n - \theta_{n-1})| dG(\theta_n) .$$

However, the range of support is tricky. $(\theta_n | z^{(n-1)})$ is the angle of ℓ_n, the line on which Z_n, the next side of the polygon, will lie. The information conditioned on is that $z^{(n-1)}$ is already part of the polygon. This restricts the range of $(\theta_n | z^{(n-1)})$ to be that where ℓ_n does not cut back through the polygon.

Define d_{n-1} to be the diagonal from v_1 to v_n, and α_{n-1} to be the angle from d_{n-1} to the horizontal at v_n. See Figure 2.3.

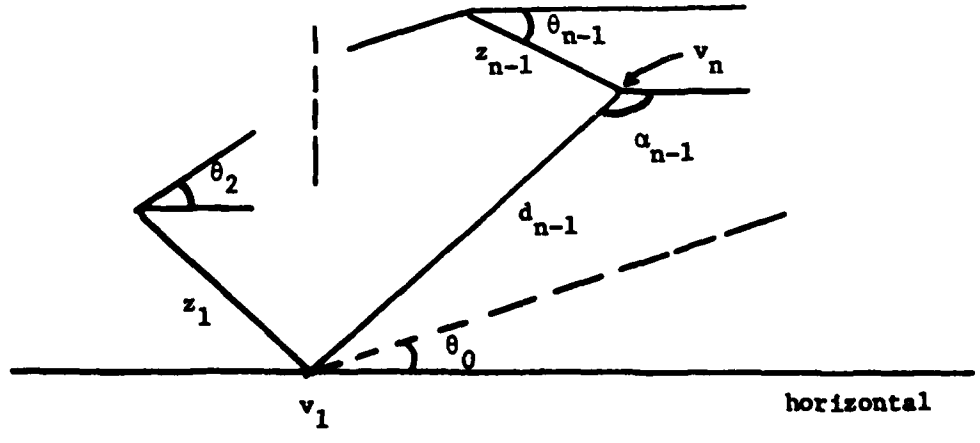

Figure 2.3.

The range of support is then

$$\theta_n \in (\alpha_{n-1}, \theta_{n-1}) \quad [10]. \tag{2.11}$$

The density on this range is

$$\begin{aligned} dF_{\theta_n | z^{(n-1)}}(\theta_n) &= dF_{\theta_n | \theta_n \in (\alpha_{n-1}, \theta_{n-1})}(\theta_n) \\ &= (q(z_{n-1}, \theta^{(n-1)}))^{-1} \sin(\theta_{n-1} - \theta_n) dG(\theta_n) \end{aligned} \tag{2.12}$$

where

$$q(z_{n-1}, \theta^{(n-1)}) = \int_{\alpha_{n-1}}^{\theta_{n-1}} \sin(\theta_{n-1} - \theta)\, dG(\theta) \tag{2.13}$$

and

$$\alpha_n = \tan^{-1} \frac{y_n}{x_n} - \pi \tag{2.14}$$

where (x_n, y_n) are the Cartesian coordinates of v_{n+1} given by (2.5).

(Note: We have written q as a function of two arguments for convenience in our use of it later).

2.6. The Conditional Distribution for General $(Z_n|\theta^{(n-1)})$.

We now derive the conditional distribution of the side lengths in the curling process. We begin with the simple but illuminating case of $(Z_1|\theta^{(1)})$. By Theorem 1.2.2 and characterization (A.2) (appendix), the distances between points of intersections along a line in $\mathcal{L}$, are independent and identically exponentially distributed with parameter $\tau\lambda(\theta)$, where θ is the orientation of the line. Thus, the distribution of $Z_1|\theta^{(n-1)}$ is

$$dF_{Z_1|\theta^{(1)}}(z_1) = \tau\lambda(\theta_1)\exp\{-\tau\lambda(\theta_1)z_1\}dz_1 \tag{2.15}$$

where $z_1 \in [0,\infty)$ and $\lambda(\theta_1)$ is given by (1.18).

For the more complicated general case, consider the triangle T with side lengths d_{n-1}, z and d with angle orientation α_{n-1}, θ_n and α respectively. See Figure 2.4.

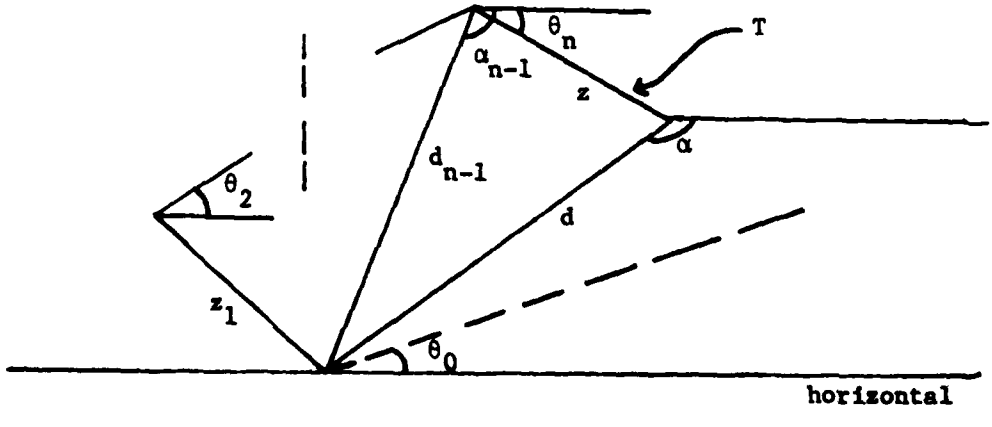

Figure 2.4.

By Theorem 1.2.4, the number of lines hitting T but not side d_{n-1} has a Poisson distribution with mean

$$\frac{\tau}{2}\,(z\lambda(\theta_n) + d\lambda(\alpha) - d_{n-1}\lambda(\alpha_{n-1}))$$

from (1.27) and using (1.18) and (2.14)

Hence, (see Snyder (1975), Chapter 2), the number of hits along ℓ_n, the line coincident with z, not crossing d_{n-1} is a non-homogeneous (linear) Poisson process with intensity $\phi(z)$ where $\phi(z)$ satisfies

$$(2.16)\qquad \frac{\tau}{2}\,[z\lambda(\theta_n) + d\lambda(\alpha) - d_{n-1}\lambda(\alpha_{n-1})] = \int_0^z \phi(z)dz\ .$$

This implies

$$(2.17)\qquad \phi(z) = \frac{\tau}{2}\,[\lambda(\theta_n) + \frac{\partial d\lambda(\alpha)}{\partial z}]\ ,$$

since d and α are functions of z, and $d\lambda(\alpha)$ evaluated at $z = 0$ is equal to $d_{n-1}\lambda(\alpha_{n-1})$.

It now follows immediately from the above, (see Snyder (1975)), that $(z_n|\theta^{(n)})$, the distance until a first hit through ℓ_n not intersecting d_{n-1}, has density

$$(2.18)\quad dF_{z_n|\theta^{(n)}}(z_n) = \phi(z_n)\exp\{-\int_0^{z_n}\phi(z)dz\}dz_n$$

$$= \frac{\tau}{2}\,[\lambda(\theta_n) + \frac{\partial d_n\lambda(\theta_n)}{\partial z_n}]\exp\{-\frac{\tau}{2}\,[z_n\lambda(\theta_n) + d_n\lambda(\alpha_n) - d_{n-1}\lambda(\alpha_{n-1})]dz_n$$

with support on $z_n \in [0,\infty)$.

We now derive a useful and surprising fact, namely that

$$\phi(z_n) = \frac{\tau}{2}\left[\lambda(\theta_n) + \frac{\partial d_n \lambda(\theta_n)}{\partial z_n}\right] = \tau q(z_n, \theta^{(n)}) \,, \tag{2.19}$$

where $q(z_n, \theta^{(n)})$ is defined in (2.13) as the measure of the set of lines in R^2 crossing ℓ_n at z_n which do not cross d_{n-1}. (2.19) says that the intensity of the nonhomogeneous Poisson process of hits along ℓ_n is proportional to $q(z_n, \theta^{(n)})$ the measure of 'available lines at z_n'.

We now proceed to derive (2.19). We begin with the trigonometric reduction

$$\begin{aligned}
\sin(\theta-\alpha_n) &= \sin(\theta - \tan^{-1}(\frac{y_n}{x_n}) + \pi) \\
&= -\sin(\theta - \tan^{-1}(\frac{y_n}{x_n})) \\
&= \frac{y_n \cos\theta - x_n \sin\theta}{(x_n^2 + y_n^2)^{1/2}} \,,
\end{aligned}$$

which combined with $d_n = (x_n^2 + y_n^2)^{1/2}$ yields

$$\begin{aligned}
d_n \lambda(\theta_n) &= d_n \int_{\alpha_n}^{\alpha_n + \pi} \sin(\theta-\alpha_n)\, dG(\theta) \\
&= \int_{\alpha_n}^{\alpha_n + \pi} (y_n \cos\theta - x_n \sin\theta)\, dG(\theta)
\end{aligned} \tag{2.20}$$

By the chain rule,

$$\frac{\partial d_n\lambda(\alpha_n)}{\partial z_n} = \frac{\partial d_n\lambda(\alpha_n)}{\partial \alpha_n} \cdot \frac{\partial \alpha_n}{\partial z_n} + \frac{\partial d_n\lambda(\alpha_n)}{\partial y_n} \cdot \frac{\partial y_n}{\partial z_n} + \frac{\partial d_n\lambda(\alpha_n)}{\partial x_n} \cdot \frac{\partial x_n}{\partial z_n} \ .$$

Evaluating the partial derivatives of $d_n\lambda(z_n)$ above via (2.20), we have

$$\frac{\partial}{\partial \alpha_n} \int_{\alpha_n}^{\alpha_n+\pi} (y_n\cos\theta - x_n\sin\theta)dG(\theta) = \frac{\partial}{\partial \alpha_n} \int_0^{\pi} |y_n\cos\theta - x_n\sin\theta|dG(\theta)$$

$$= 0$$

$$\frac{\partial}{\partial y_n} \int_{\alpha_n}^{\alpha_n+\pi} (y_n\cos\theta - x_n\sin\theta)dG(\theta) = \int_{\alpha_n}^{\alpha_n+\pi} \cos\theta \, dG(\theta)$$

$$\frac{\partial}{\partial y_n} \int_{\alpha_n}^{\alpha_n+\pi} (y_n\cos\theta - x_n\sin\theta)dG(\theta) = \int_{\alpha_n}^{\alpha_n+\pi} \sin\theta \, dG(\theta)$$

where the last two partials follow by Leibnitz's rule. From (2.5) we have

$$\frac{\partial y_n}{\partial z_n} = \sin\theta_n \ , \ \frac{\partial x_n}{\partial z_n} \cos\theta_n \ .$$

Combining the above we obtain

$$\frac{\partial d_n\lambda(\alpha_n)}{\alpha z_n} = \int_{\alpha_n}^{\alpha_n+\pi} (\sin\theta_n\cos\theta - \cos\theta_n\sin\theta)dG(\theta)$$

$$= \int_{\alpha_n}^{\alpha_n+\pi} \sin(\theta_n-\theta) \, dG(\theta) \ .$$

But then

$$\phi(z) = \frac{\tau}{2}\left[\lambda(\theta_n) + \frac{\partial d_n \lambda(\alpha_n)}{\partial z_n}\right]$$

$$= \frac{\tau}{2}\left[\int_{\theta_n}^{\theta_n+\pi} \sin(\theta-\theta_n)dG(\theta) + \int_{\alpha_n}^{\alpha_n+\pi} \sin(\theta_n-\theta)dG(\theta)\right]$$

$$= \frac{\tau}{2}\left[-\int_{\alpha_n+\pi}^{\theta_n+\pi} \sin(\theta_n-\theta)dG(\theta) + \int_{\alpha_n}^{\theta_n} \sin(\theta_n-\theta)dG(\theta)\right]$$

$$= \frac{\tau}{2}\left[\partial \int_{\alpha_n}^{\theta_n} \sin(\theta_n-\theta)dG(\theta)\right]$$

$$= \tau\, q(z_n, \theta^{(n)}) ,$$

which verifies (2.19).

Combining (2.18) with (2.19) we obtain another useful expression for the density of $(Z_n|\theta^{(n)})$, namely

$$(2.21) \quad dF_{Z_n|\theta^{(n)}}(z_n) = \tau\, q(z_n,\theta^{(n)})\exp\{-\frac{\tau}{2}\left[z_n\lambda(\theta_n) + d_n\lambda(\alpha_n) - d_{n-1}\lambda(\alpha_{n-1})\right]\}dz_n .$$

(2.21) fits nicely with the angle density (2.12) to provide, as we will see, a substantially simplified joint density.

We rewrite (2.18) one more way which will be extremely useful in deriving fast algorithms for simulating the curling process in Chapter 4. By (2.18) and (2.19) again,

$$(2.22) \quad dF_{Z_n|\theta^{(n)}}(z_n) = \tau\, q(z_n,\theta^{(n)})\exp\{-\tau\, Q(z_n,\theta^{(n)})\}dz_n ,$$

where

$$Q(Z_n,\theta^{(n)}) = \int_0^{Z_n} q(z,\theta^{(n)})dz \ . \tag{2.23}$$

We remind the reader that the support of (2.21) and (2.22) is $[0,\infty)$.

2.7. The Joint Density of $Z^{(n)}$ - The Curling Process.

We summarize and conclude this chapter with the joint density of $Z^{(n)}$. This is obtained simply as the product of the conditional densities

$$dF_{Z^{(n)}}(z^{(n)}) = dF_{\Theta_0,\Theta_1}(\theta_0,\theta_1) \cdot dF_{Z_1|\theta^{(1)}}(z_1) \cdot dF_{\Theta_2|z^{(1)}}(\theta_2)$$

$$\cdots dF_{\Theta_n|z^{(n-1)}}(\theta_n) \cdot dF_{Z_n|\theta^{(n-1)}}(z_n) \cdot$$

Summarizing the previous results, we have from (2.7)

$$dF_{\Theta_0,\Theta_1}(\theta_0,\theta_1) = \frac{2}{\lambda} \sin(\theta_1-\theta_0)\, dG(\theta_0)\, dG(\theta_1) \tag{2.24}$$

$$\text{on} \quad 0 \le \theta_0 < \theta_1 \le \pi ,$$

from (2.12)

$$dF_{\Theta_n|z^{(n-1)}}(\theta_n) = (q(z_{n-1},\theta^{(n-1)}))^{-1} \sin(\theta_{n-1}-\theta_n)\, dG(\theta_n) \tag{2.25}$$

$$\text{on} \quad \alpha_{n-1} < \theta_n < \theta_{n-1} ,$$

and from (2.21)

$$dF_{Z_n|\theta^{(n)}}(z_n) = \tau\, q(z_n,\theta^{(n)}) \cdot \exp\{-\tfrac{\tau}{2}\,[z_n\lambda(\theta_n) + d_n\lambda(\alpha_n) - d_{n-1}\lambda(\alpha_{n-1})]\}dz_n \tag{2.26}$$

$$\text{on} \quad 0 \le z_n < \infty .$$

Thus,

$$(2.27)\qquad dF_{Z^{(n)}}(z^{(n)}) = -\frac{2}{\lambda}\left(\prod_{i=1}^{n}\sin(\theta_i-\theta_{i-1})\right)$$

$$\cdot\,\tau^n \exp\{-\frac{\tau}{2}\left[\left(\sum_{i=1}^{n} z_i\lambda(\theta_i)\right) + d_n\lambda(\alpha_n)\right]$$

$$\cdot\, q(z_n,\theta^{(n)})\left(\prod_{i=0}^{n} dG(\theta_i)\right)\left(\prod_{i=1}^{n} dz_i\right)$$

on the set

$$(2.28)\qquad \{z^{(n)}:\quad 0 \le \theta_0 < \theta_1 \le \pi,$$

$$\alpha_{i-1} < \theta_i < \theta_{i-1} \qquad i = 2,\ldots,n\ ,$$

$$0 \le z_j < \infty \qquad j = 1,\ldots,n\}\ .$$

The support (2.28) can be expressed in different useful ways as will be seen in Chapter 3.

CHAPTER 3

POLYGON DISTRIBUTIONS

In this chapter we take the constructed curling process, and use it to derive expressions for the distribution of polygon characteristics. As was described in Section 2.3, we use a stopping time to extract polygons from the curling process. This procedure turns out to be mathematically convenient as well as efficient for the simulations in Chapter 4. We also define some general families of anisotropic distributions which are particularly appropriate for the general distributional forms obtained. Finally, in the last section, we suggest some alternative approaches to obtaining distributional information from the curling process.

3.1. The Polygon Formed by the Curling Process.

(Here and in the rest of this chapter we shall find it necessary to distinguish in our notation between the curling process and the polygon formed. We shall do so by placing a '~' over the curling process coordinates as described in Section 2.4.)

Selecting θ_1 and θ_0 at the beginning of the curling process is tantamount to selecting ℓ_1 and $\ell_0 = \ell_N$, the two lines coincident with the first and last edges, z_1 and z_N, of the polygon sampled. However, whereas the curling process 'travels' over ℓ_1, there is

no edge of the curling process on ℓ_0. The polygon 'formed' by the curling process has as its boundary the curling process realization up to the first intersection with ℓ_0, together with the length along ℓ_0 from v_1 to this intersection point. This point becomes the last vertex of the polygon v_N, and the last side of the polygon z_N, becomes this length along ℓ_0 from v_1 to v_N. See Figure 3.1.

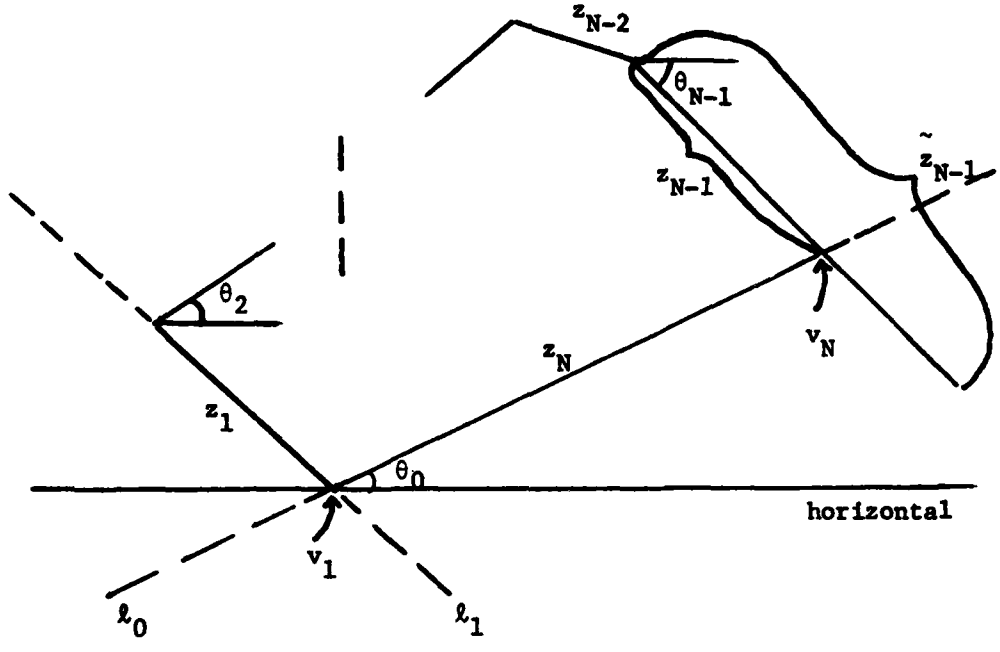

Figure 3.1.

3.2. The Event $\{N = n\}$.

N, the number of sides of the polygon formed, is one more than the index of the first side length of the curling process to cross ℓ_0. That is,

$$N = \inf\{n: \sum_{i=1}^{n-1} \tilde{Z}_i \sin(\tilde{\Theta}_1 - \tilde{\Theta}_0) < 0\} \quad . \tag{3.1}$$

Precisely, N-1 is a stopping time of the curling process (in the sequence $\{(\Theta_n, Z_n)\}$ of angle and side pairs).

The event $\{N = n\}$ can be usefully expressed as

$$\begin{aligned} \{N = n\} &= \{N > n-1 \text{ and } \tilde{Z}_{n-1} \text{ crosses } \ell_0\} \\ &= \{N > n-1 \text{ and } \tilde{\Theta}_{n-1} < \tilde{\Theta}_0 \text{ and } \tilde{Z}_{n-1} > \tilde{U}_{n-1}\} \end{aligned} \tag{3.2}$$

where we define

$$\tilde{U}_k = -\sec(\tilde{\Theta}_k - \tilde{\Theta}_0) \sum_{i=1}^{k-1} \tilde{Z}_i \sin(\tilde{\Theta}_i - \tilde{\Theta}_0) \ . \tag{3.3}$$

The requirement that $\tilde{\Theta}_{n-1} < \tilde{\Theta}_0$ in (3.2) is necessary and sufficient for $\tilde{Z}_{n-1}$ to cross ℓ_0 when $\tilde{Z}_{n-1} > \tilde{U}_{n-1}$.

We can use (3.2) and the joint density (2.27) to find, in principle, the distribution of N by

$$P\{N=n\} = \int_{\{N=n\}} dF_{\tilde{Z}^{(n-1)}}(z^{(n-1)}) \ . \tag{3.4}$$

This integration, as we will see, is in most cases, prohibitively difficult to carry out.

We now proceed to describe each set $\{N=n\}$ in terms of an explicit range of $z^{(n-1)}$ (actually R^{2n-1}) where the integration in (3.4) might be carried out. For $m = 2,\ldots,n-1$, define

$$(3.5)\qquad D_m^{(n)} = \{\theta^{(n)}: \theta_0 \le \theta_i < \theta_{i-1},\ 0 \le z_i < \infty \text{ for } i=1,\ldots,m-1$$

$$\text{and}\quad \alpha_{m-1} < \theta_m < \theta_0,\ 0 \le z_m < u_m$$

$$\text{and}\quad \alpha_{j-1} < \theta_j < \theta_{j-1},\ 0 \le z_j < u_j \text{ for } j=m+1,\ldots,n-1$$

$$\text{and}\quad \alpha_{n-1} < \theta_n < \theta_{n-1}\},$$

and

$$(3.6)\qquad D_n^{(n)} = \{\theta^{(n)}: \theta_0 \le \theta_i < \theta_{i-1},\ 0 \le z_i < \infty \text{ for } i=1,\ldots,n-1$$

$$\text{and}\quad \alpha_{n-1} < \theta_n < \theta_0\},$$

and

$$(3.7)\qquad D^{(n-1)} = \bigcup_{m=2}^{n-1} D_m^{(n-1)}.$$

(Note: α_k is as in (2.14) and u_k corresponds to $\tilde{U}_k$ in (3.3)).

Thus

$$\{N=n\} = D^{(n-1)} \cap \{z^{(n-1)}: u_{n-1} \leq z_{n-1} < \infty\} . \tag{3.8}$$

(3.8) follows from (3.2) as can be verified by induction.

An immediate observation from this section is the result that the distribution of N is in general invariant under changes in the intensity parameter τ. This follows by observing that transforming $z_i' = \tau z_i$, $i = 1,\ldots,n$ in (2.27) yields a density not depending on τ. Furthermore, the sets $\{N=n\}$ are unchanged by such a transformation as can be seen by examination of (3.5) and (3.6). The result then follows from (3.4).

We might remark here about our future notational use of N as an index. Any variable indexed by N is defined to be that variable indexed by n on the set $\{N=n\}$. For example,

$$\theta^{(N-1)} = \sum_{n=3}^{\infty} \theta^{(n-1)} \cdot I\{N=n\} . \tag{3.9}$$

3.3. The Joint Density of Z(N) of Polygons.

It was pointed out in Section 2.2 that N and $\theta^{(N-1)}$ specify a polygon up to translation since the last three polygon coordinates Z_{N-1}, θ_N and Z_N are determined by $\theta^{(N-1)}$ via the relationships in (2.3). Hence, the distribution of $\theta^{(N-1)}$ is equivalent to that of $Z^{(N)}$. We now derive the distribution of $\theta^{(N-1)}$ from the curling process.

Figure 3.1 illustrates quite clearly that the curling process coordinates and the polygon coordinates are identical until the curling process crosses ℓ_0, at which point they depart. More precisely we have,

$$\tilde{\theta}^{(N-1)} = \theta^{(N-1)} \quad \text{but} \quad \tilde{Z}_{N-1} \neq Z_{N-1} \ (\text{w.p.1}) \tag{3.10}$$

By (3.9) and (3.10), we can specify the density of $\theta^{(N-1)}$ by the densities of $\tilde{\theta}^{(n-1)}$ on the sets $\{N = n\}$. Expressing $\{N = n\}$ by (3.8) we obtain

$$dF_{\theta^{(N-1)}}(\theta^{(n-1)}) = \int_{u_{n-1} \leq z_{n-1} < \infty} dF_{\tilde{Z}^{(n-1)}}(z^{(n-1)}) \tag{3.11}$$

with support on $D^{(n-1)}$.

By (2.19) and (2.27) the right side of (3.11) is

$$(3.12)\qquad -\frac{2}{\lambda}\Big(\prod_{i=1}^{n-1}\sin(\theta_i-\theta_{i-1})\Big)\tau^{n-2}$$
$$\cdot\exp\Big\{-\frac{\tau}{2}\sum_{i=1}^{n-2}z_i\lambda(\theta_i)\Big\}\Big(\prod_{i=0}^{n-1}dG(\theta_i)\Big)\Big(\prod_{i=1}^{n-2}dz_i\Big)$$
$$\cdot\int_{u_{n-1}}^{\infty}\frac{\tau}{2}\Big[\lambda(\theta_{n-1})+\frac{\partial d_{n-1}\lambda(\alpha_{n-1})}{\partial z_{n-1}}\Big]$$
$$\cdot\exp\Big\{-\frac{\tau}{2}\big[z_{n-1}\lambda(\theta_{n-1})+d_{n-1}\lambda(\alpha_{n-1})\big]\Big\}dz_{n-1}\,.$$

The definite integral on the right side of (3.12) is evaluated as

$$(3.13)\qquad -\exp\Big\{-\frac{\tau}{2}\big[z_{n-1}\lambda(\theta_{n-1})+d_{n-1}\lambda(\theta_{n-1})\big]\Big\}\Big|_{u_{n-1}}^{\infty}$$
$$=\exp\Big\{-\frac{\tau}{2}\big[z_{N-1}\lambda(\theta_{N-1})+z_N\lambda(\theta_N)\big]\Big\}$$

since

$$(3.14)\qquad \text{on}\ \{N=n\}\,,\ u_{n-1}=z_{N-1}\,,\ d_n=z_N\ \text{and}\ \alpha_{n-1}=\theta_N\,.$$

Combining (3.11)-(3.13), we have on $\{N=n\}$

$$(3.15)\qquad dF_{\theta^{(N-1)}}(\theta^{(n-1)})=-\frac{2}{\lambda}\Big(\prod_{i=1}^{n-1}\sin(\theta_i-\theta_{i-1})\Big)\tau^{n-2}$$
$$\cdot\exp\Big\{-\frac{\tau}{2}\Big[\sum_{i=1}^{n}z_i\lambda(\theta_i)\Big]\Big\}\Big(\prod_{i=0}^{n-1}dG(\theta_i)\Big)\Big(\prod_{i=1}^{n-2}dz_i\Big)$$

with support on $D^{(n-1)}$.

We now extend (3.15) to define a general density on $\mathbb{R}^\infty$ which corresponds to the density of polygons in ρ^{**}. This is simply done by establishing a correspondence between cylinder sets of $\mathbb{R}^\infty$ and the events $\{N=n\}$. We then obtain $dF_{Z^{(N)}}$ as $dF_{\theta^{(N-1)}}$ on those sets and zero elsewhere.

More precisely, let $z = (\theta_0,\theta_1,z_1,\theta_2,z_2,\ldots)$ denote a point in $\mathbb{R}^\infty$. Define $Z^{(n)} \subset \mathbb{R}^\infty$ such that

$$Z^{(n)} = \{z: \theta^{(n-1)} \in D^{(n-1)} \text{ and } z^{(n)} \text{ satisfies (2.3)}\} . \tag{3.16}$$

Since $Z^{(n)} \cap Z^{(m)} = \phi$ for $n \neq m$, and since $\{N = n\} = Z^{(n)}$, we have from (3.9),

$$dF_{Z^{(N)}}(z) = \sum_{n=3}^{\infty} dF_{\Theta^{(N-1)}}(\theta^{(n-1)}) \cdot I\{z \in Z^{(n)}\} . \tag{3.17}$$

That (3.17) contains differential elements of varying length $2N-2$ may seem awkward. However, it does express very nicely that the dimension of the density $dF_{Z^{(N)}}$ is varying over the cylinder sets $Z^{(n)}$. This is simply a restatement of the fact that an N sided polygon is determined (up to translation) by $2N-2$ coordinates.

We summarize the results of this section by combining (3.15)-(3.17) into

$$dF_{Z^{(N)}}(z) = -\frac{2}{\lambda}\left(\prod_{i=1}^{N-1} \sin(\theta_i-\theta_{i-1})\right)\tau^{N-2} \tag{3.18}$$

$$\cdot \exp\{-\frac{\tau}{2}\left[\sum_{i=1}^{N} z_i\lambda(\theta_i)\right]\}\left(\prod_{i=0}^{N-1} dG(\theta_i)\right)\left(\prod_{i=0}^{N-2} dz_i\right) ,$$

where $z \in Z^{(n)} \Rightarrow N = n$. $dF_{Z^{(N)}}(z)$ is taken to have support only on $Z = \bigcup_{n=3}^{\infty} Z^{(n)}$.

We observe an immediate fact from (3.18) concerning the distribution of S and A under changes in τ. The transformation $z_i = \tau z_i$, $i = 1,\ldots,N$, yields the distribution of polygons for $\tau = 1$. If we denote by $S(\tau)$ and $A(\tau)$, the distributions of S and A under intensity τ, then this transformation coupled with (2.4) and (2.6) yields $S(\tau) = \tau S(1)$ and $A(\tau) = \tau^2 A(1)$. Thus, the distribution of $S(\tau)$ and $A(\tau)$ are easily obtainable from the distributions of $S(1)$ and $A(1)$.

3.4. The Polygon Density in Isotropic ρ^{**}.

For isotropic ρ^{**}, we have $dG(\theta) = \frac{1}{\pi}\, d\theta$, from (1.13), and $\lambda(\theta) \equiv \frac{2}{\pi}$ from (1.20). As we mentioned in Section 2.4, we take $\theta_0 \equiv 0$ and use the marginal density in (2.10) for dF_{θ_1}. Thus, the density (3.18) becomes

$$(3.19) \qquad dF_{Z(N)}(z) = \left(\frac{\pi-\theta_1}{\pi}\right)\left(\prod_{i=1}^{N-1} \sin(\theta_{i-1}-\theta_i)\right)\left(\frac{\tau}{\pi}\right)^{N-2} \cdot \exp\{-\frac{\tau}{\pi}\, s\}\left(\prod_{i=1}^{N-2} d\theta_i dz_i\right) d\theta_{N-1}$$

with support on $\mathcal{Z}$. ($s = \sum_{i=1}^{n} z_i$ as in (2.4)).

By suitable reparametrization the isotropic density (3.19) can be shown to be the same as the isotropic ergodic density derived by Miles (1973) [11]. This agreement means that independent realizations of the curling process yield the equivalent of an i.i.d. sample of polygons from the ergodic distribution. We should remark that ergodicity of the Poisson line process implies that the ergodic distribution of polygons is the same in any ρ^* (w.p.1). Hence the distribution of polygons in ρ^{**} will necessarily be identical with the ergodic distribution of polygons in any ρ^* (w.p.1) if the ergodic distribution is suitably defined.

3.5. The Distribution of Polygon Characteristics in Isotropic ρ^{**}.

Before demonstrating how one can (in principle) derive the distributions of N, S and A in isotropic ρ^{**}, we remark that some of the moments of these distributions are known. Some of these are

$$
(3.20)\quad \begin{cases} E[N] = 4 & E[S] = 2\tau/\pi & E[A] = \pi/\tau^2 \\ E[N^2] = (\pi^2+24)/2 & & \\ E[SN] = \pi(\pi^2+8)/2\tau & E[S^2] = \pi^2(\pi^2+4)/2\tau^2 & \\ E[AN] = \pi^3/2\tau^2 & E[AS] = \pi^4/2\tau^3 & E[A^2] = \pi^4/2\tau^4 \\ E[NA^2] = \pi^4(8\pi^2-21)/21\tau^4 & E[SA^2] = 8\pi^7/21\tau^5 & E[A^3] = 4\pi^7/7\tau^6 \,. \end{cases}
$$

(3.20) and other moment results have been derived by R. Miles, D. G. Kendall, P. I. Richards and H. Solomon with ad hoc techniques. Miles (1973) and Solomon (1978) contain explicit illustrations of some of these derivations. Generalizing these techniques to find higher order moments unfortunately seems to yield irreducible integral formulas. An example of such difficulty is provided in Appendix A.2 where the author has derived an integral formula for $E[A^4]$. It is interesting to note that $E[N]$, $E[A]$ and $E[A^2]$ above, agree (after normalization) with the results derived by Goudsmit (1945).

The reasonably simple closed form expressions in (3.20) lead one to believe that similarly simple analytical expressions exist for the joint and marginal distributions of N, S and A. To date, as far as the author knows, no one has succeeded in finding them. We now carry

out explicitly some of the manipulations of the density (3.19) to demonstrate some of what is known about these distributional forms.

Having already carried out the integration of (3.4) over z_{n-1} in (3.13), the distribution of N is expressed from (3.19) as

$$P\{N=n\} = \int_{Z^{(n)}} dF_{Z^{(N)}}(z) \ . \tag{3.21}$$

For $n = 3$, (3.21) becomes

$$P\{N=3\} = \int_0^\infty \int_{\theta_1-\pi}^0 \int_0^\infty \frac{(\pi-\theta_1)}{\pi} \sin\theta_1 \sin(\theta_1-\theta_2) \cdot \frac{\tau}{\pi} \exp\{-\frac{\tau}{\pi} z_1[1+\cos\theta_1 - \sin\theta_1(\frac{1+\cos\theta_2}{\sin\theta_2})]\} \, dz_1 d\theta_2 d\theta_1 \ . \tag{3.22}$$

The exponent in (3.22) is arrived at by the relationship

$$s = \sum_{i=1}^{N} z_i = \sum_{i=1}^{N-2} z_i[1+\cos\theta_i - \sin\theta_i(\frac{1+\cos\theta_{N-1}}{\sin\theta_{N-1}})] \tag{3.23}$$

derivable from (2.3) when $\theta_0 = 0$.

By Fubini, we elect to first integrate out z_1 in (3.22) to obtain

$$\frac{1}{\pi} \int_0^\pi \int_{\theta_1-\pi}^0 (\pi-\theta_1) \frac{\sin\theta_1 \sin\theta_2 \sin(\theta_1-\theta_2)}{\sin\theta_2 - \sin\theta_1 - \sin(\theta_1-\theta_2)} \, d\theta_2 d\theta_1 \ . \tag{3.24}$$

Simplification of the integrand in (3.24) requires the trigonometric identities

$$(3.25)\qquad \sin\theta_1\sin\theta_2\sin(\theta_1-\theta_2) = 8\left(\sin\frac{\theta_1}{2}\cos\frac{\theta_1}{2}\sin\frac{\theta_2}{2}\cos\frac{\theta_2}{2}\right) \cdot \sin\left(\frac{\theta_1-\theta_2}{2}\right)\cos\left(\frac{\theta_1-\theta_2}{2}\right)$$

and

$$(3.26)\qquad \sin\theta_2 - \sin\theta_1 - \sin(\theta_1-\theta_2) = -4\sin\left(\frac{\theta_1-\theta_2}{2}\right)\left(\cos\frac{\theta_1}{2}\cos\frac{\theta_2}{2}\right) .$$

(3.25) and (3.26) reduce (3.24) to

$$-\frac{2}{\pi}\int_0^{\pi}\int_{\theta_1-\pi}^{0}(\pi-\theta_1)\cos\left(\frac{\theta_1}{2}-\frac{\theta_2}{2}\right)\sin\frac{\theta_1}{2}\sin\frac{\theta_2}{2}\,d\theta_2 d\theta_1$$

which can be evaluated by elementary calculus techniques to yield

$$(3.27)\qquad P\{N=3\} = 2 - \frac{\pi^2}{6} \approx 0.3551$$

a result previously derived by Miles (1964).

The derivation of $P\{N=3\}$ above, although straightforward, is by no means a trivial calculation. For $P\{N=4\}$, integration over $Z^{(4)}$ requires separate integrations over D_2^3 and D_3^3 defined in (3.5) and (3.6). Through Fubini, we can integrate out z_1 and z_2 first to reduce five-fold integrals to three-fold integrals. Unfortunately, these three-fold integrals do not seem to yield closed form solutions and must be evaluated by numerical methods. We substitute the Monte Carlo approximations in Chapter 4 for the numerical integration.

The distributions of S and A should be obtainable (in principle) from (3.19) with appropriate transformations involving the expressions (2.4) and (2.6). The author however, has not yet found a transformation that yields a tractable integral. Miles (1973) is able to derive a partial result in this direction. He suggests the transformation

$$z_1 \to s\,, \quad z_2 \to \xi_i s \qquad i = 2,\ldots,N$$

which in our case reduces (3.19) to

$$(3.28) \qquad [(\frac{\tau}{\pi})^{N-2} s^{N-3} e^{-\frac{\tau}{\pi} s}\, ds][(\frac{\pi-\theta_1}{\pi})(\prod_{i=1}^{N-1} \sin(\theta_i-\theta_{i-1}))$$

$$(\frac{\sin\theta_{N-1}}{\xi_2 \cos\theta_1(\sin\theta_2 + \cot\theta_{N-1}\cos\theta_2)})(\prod_{i=3}^{N-1} d\theta_i)(\prod_{i=2}^{N} d\lambda_i)]\,.$$

Let $\psi = (\theta_3,\ldots,\theta_{N-1},\xi_2,\ldots,\xi_N)$, so that ψ determines the 'shape' of the polygon. Given N, the ranges of S and ψ do not depend on each other. Thus (3.28) implies that given N, $2\tau S/\pi$ is χ^2 distributed with $2(N-2)$ degrees of freedom. Miles also observes that given N, S and ψ are independent, inotherwords the perimeter and the shape are independent within each class of polygons of a fixed number of sides.

We are able to make one more conclusion from (3.28). Since the intensity τ does not appear on the right, then given N, the distribution of ψ does not depend on τ. But we know from Section 3.2 that the distribution of N does not depend on τ. We conclude that the distribution of 'shapes' of polygons, ψ, in isotropic ρ^{**}, is invariant under changes in the intensity parameter τ.

3.6. The Polygon Densities for Families of Anisotropic ρ^{**}.

Specification of the density of polygons (3.18) for particular anisotropic ρ^{**} requires $dG(\theta)$ and $\lambda(\theta)$ for $\theta \in [0,\pi)$. Given G, the calculation of $\lambda(\theta^*)$ is as follows. From (1.18),

$$\lambda(\theta^*) = \int_0^{\pi} |\sin(\theta-\theta^*)| dG(\theta)$$

$$= \int_0^{\theta_*} (-\cos\theta^* \sin\theta + \sin\theta^* \cos\theta)\, dG(\theta)$$

$$+ \int_{\theta_*}^{\pi} (\cos\theta^* \sin\theta - \sin\theta^* \cos\theta)\, dG(\theta) .$$

Thus for the indefinite integral

$$F(\theta) = \int (\cos\theta^* \sin\theta - \sin\theta^* \cos\theta)\, dG(\theta) \tag{3.29}$$

we have

$$\lambda(\theta^*) = F(\pi) + F(0) - 2F(\theta^*) . \tag{3.30}$$

Obtaining F and hence $\lambda(\theta^*)$ in closed form from (3.29) and (3.30) is not always an easy matter. [12]

We now propose a family $\mathcal{G}^C$ of continuous densities on $[0,\pi)$ which are general, interpretable and yield $\lambda(\theta^*)$ in closed form. Simple expressions for $\lambda(\theta^*)$ give us simpler polygon densities and make for simpler, faster and more accurate simulations of the curling process,

as we will see in Chapter 4. Define

(3.31) $$\mathcal{G}^C = \{G: G \text{ is of the form (3.32)}\}$$

(3.32) $$dG_{(n,m,\alpha,\beta)}(\theta) = K^{-1} \sum_{i=1}^{n} \beta_i |\sin^{m_i}(\theta-\alpha_i)|\, d\theta$$

for $\theta \in [0,\pi)$, where

(3.33)
$$\begin{cases} (n,m,\alpha,\beta) = (n,m_1,\ldots,m_n,\alpha_1,\ldots,\alpha_n,\beta_1,\ldots,\beta_n) \\ n \in \{0,1,2,\ldots\} \\ m_i \in \{0,1,2,\ldots\} \\ \alpha_i \in [-\frac{\pi}{2}, \frac{\pi}{2}) \\ \beta_i \in (0,\infty) \\ K = \sum_{i=1}^{n} \beta_i K_{m_i} \\ \text{where } K_m = \int_0^{\pi} \sin^m \theta\, d\theta = \pi^{1/2} \dfrac{\Gamma(\frac{m+1}{2})}{\Gamma(\frac{m}{2}+1)} . \end{cases}$$

The interpretation of $G_{(n,m,\alpha,\beta)}$ is as a mixture of

(3.34)
$$\begin{cases} n \text{ pulses in } [0,\pi) \text{ with} \\ m_i = \text{sharpness of the } i^{th} \text{ pulse} \\ \alpha_i + \frac{\pi}{2} = \text{location of the } i^{th} \text{ pulse} \\ \beta_i = \text{relative size of the } i^{th} \text{ pulse} . \end{cases}$$

Notice that $(m_1,\ldots,m_n) = (0,\ldots,0)$ yields isotropic G. We write $G_{(0)}$ for such G.

The intuitive interpretability (3.34) suggests that $\mathcal{G}-G_{(0)}$ is a useful family of alternatives to isotropy, especially for statistical analysis. We show in A.2 of the appendix that $\mathcal{G}$ is dense in the class of continuous probability densities on $[0,\pi]$ so that $\mathcal{G}$ essentially contains all alternatives. Finally, the functions $\lambda(\theta^*)$ obtained from members of $\mathcal{G}$ are in closed form as we show below.

Define for general $G \in \mathcal{G}$

$$\lambda_{(n,m,\alpha,\beta)}(\theta^*) = \int_0^\pi |\sin(\theta-\theta^*)| dG_{(n,m,\alpha,\beta)}(\theta) \tag{3.35}$$

and for the special case

$$\lambda_m(\theta^*) = \lambda_{(1,m,0,1)}(\theta^*) . \tag{3.36}$$

The following relationship substantially reduces the computational effort for finding general λ.

$$\lambda_{(n,m,\alpha,\beta)}(\theta^*) = K^{-1} \sum_{i=1}^{n} \beta_i K_{m_i} \lambda_{m_i}(\theta^*-\alpha_i) . \tag{3.37}$$

We derive (3.37) as follows

$$\lambda_{(n,m,\alpha,\beta)}(\theta^*) = K^{-1} \int_0^{\pi} |\sin(\theta-\theta^*)\ |(\sum_{i=1}^{n} \beta_i |\sin^{m_i}(\theta-\alpha_i)|)d\theta$$

$$= K^{-1} \sum_{i=1}^{n} \beta_i \int_0^{\pi} |\sin(\theta-\theta^*)||\sin^{m_i}(\theta-\alpha_i)|\, d\theta$$

$$= K^{-1} \sum_{i=1}^{n} \beta_i \int_0^{\pi} |\sin(\theta-(\theta^*-\alpha_i))|\sin^{m_i}\theta\, d\theta$$

$$= K^{-1} \sum_{i=1}^{n} \beta_i K_{m_i} \lambda_{m_i}(\theta^*-\alpha_i)$$

$\lambda_m(\theta^*)$ and hence general λ can be calculated by elementary methods from (3.29) and (3.30). (This is a long calculation for large m). For example,

(3.38) $$\lambda_1(\theta^*) = \frac{1}{2}\left[(\frac{\pi}{2} - \theta^*)\cos\theta^* + \sin\theta^*\right],$$

(3.39) $$\lambda_2(\theta^*) = \frac{4}{3\pi}(\cos^2\theta^* + 1)$$

and

(3.40) $$\lambda_4(\theta^*) = \frac{16}{15\pi}(1 + 2\cos^2\theta^* - \frac{1}{3}\cos^4\theta^*) .$$

We also propose the family $\mathcal{G}^D$ of discrete alternatives to isotropy defined by

(3.41) $$\mathcal{G}^D = \{G: G \text{ has a p.m.f. } g \text{ of the form (3.42)}\}$$

(3.42) $$g(\theta_i) = p_i , \quad \text{for } i = 1,\ldots,I \text{ and } \theta_i \in [0,\pi) .$$

Consisting of a finite number of discrete pulses or atoms in $[0,\infty)$, we note that

$$\lim_{\substack{m_i \to \infty \\ i=1,\ldots,I}} G_{(I,m_1,\ldots,m_I,\theta_1,\ldots,\theta_I,p_1,\ldots,p_I)}(\theta) \in \mathcal{G}^D$$

so that members of $\mathcal{G}^D$ are (pointwise) limits or extremes of members of $\mathcal{G}^C$. Thus, investigation into anisotropic ρ^{**} generated by members of $\mathcal{G}^D$ is another way of gaining insight into which alternatives to isotropy should be considered. Preliminary modelling by members of $\mathcal{G}^D$ would be a strategy to the eventual fitting of members of $\mathcal{G}^C$.

Calculation of $\lambda(\theta^*)$ for members $g \in \mathcal{G}^D$ is done directly from (1.18). Because the angles of the curling process pertain only to intersections between members of $\mathcal{L}$, we need only evaluate $\lambda(\theta^*)$ at the atoms of g. We have, for g of the form (3.42),

$$\lambda(\theta_j) = \sum_{i=1}^{I} p_i |\sin(\theta_i - \theta_j)| \ , \quad j = 1,\ldots, I \ . \tag{3.43}$$

Notice that for the discrete uniform case, (i.e. where $p_i = \frac{1}{I}$ for $i = 1,\ldots,I$), $\lambda(\theta_i) = \lambda(\theta_j)$ for all i, j in (3.43). For computer simulation of the curling process induced by $g \in \mathcal{G}^D$, we first compute and store the I necessary values of $\lambda(\theta^*)$ specified by (3.43).

In Chapter 4, we carry out a simulation study of anisotropic ρ^{**} induced by some of the simpler members of $\mathcal{G}^C$ and $\mathcal{G}^D$.

We close this section by remarking that analogous to the moment results in (3.20), Miles (1964) provides the following known first and second order moments of N, S, and A in the general anisotropic case.

$$(3.44)\quad \begin{cases} E[N] = 4 & E[S] = 4/\lambda\tau & E[A] = 2/\lambda\tau^2 \\ E[N^2] = \lambda\eta + 12 & & E[A^2] = 4\eta/\lambda\tau^2 \\ E[SN] = 2(\lambda\eta + 4)/\lambda\tau & E[AN] = 2\eta/\tau^2 & E[AS] = 4\eta/\lambda\tau^3 \end{cases}$$

where

$$(3.45)\qquad \lambda = \int_0^{\pi} \lambda(\theta)\, dG(\theta)$$

as in (1.31) and,

$$(3.46)\qquad \eta = \int_0^{\pi} [\lambda(\theta)]^{-2}\, d\theta \quad .$$

3.7. Extensions of the Curling Process.

As we have seen in this chapter, the integral expressions obtained for the joint distribution of the angles and side lengths in the general case (3.18) and even in the much simpler isotropic case (3.19) are too unwieldy for deriving the distributions of N, S or A. The approximate answers obtained by the simulation in Chapter 4 are a partial solution to this difficulty. However, it seems that more tractable expressions may be obtainable by exploiting the curling process in alternative ways. We mention some of these alternatives in this section, and suggest possible directions for future work.

The most obvious extension of the curling process is to use other stopping times. For example, by stopping at the crossing of ℓ_1 (after ℓ_0), the curling process samples two adjacent random polygons. Other stopping times sample more complicated combinations of polygons. Investigation of these related polygons would yield information concerning the association among polygons. Furthermore, the unions of adjacent polygons form other polygon aggregates. Miles (1973) has shown that the distributions of polygon characteristics in these aggregates correspond to certain weightings of the distributions in ρ^*. [12] Different stopping times for the curling process enable us to explore these aggregates.

Another alternative is to skip selection of the initial angle, (Θ_0 in the anisotropic case and Θ_1 in the isotropic case), and to begin the curling process with the next variable, (Θ_1 in the anisotropic case and Z_1 in the isotropic case). Indeed, careful examination of the conditional densities of angles and sides in (2.25) and (2.26)

reveals that these densities are independent of the initial angle. The distribution of θ_0, or θ_1 in the isotropic case, applied to this process would yield relationships among the probabilities in the distribution of N. Presumably, these relationships would be similar to the recursive integral equations alluded to by Miles (1964, 1973).

Finally we mention a method to exploit the invariance of the distribution of N under changes in the intensity τ. In the appendix, we show that this invariance yields a relationship between the distribution of N and the probabilities of splitting a random N-sided polygon by a random secant into a j-sided and an (N+4-j)-sided polygon. If the procedure to select a random secant could be incorporated into the curling process, it would be a valuable tool for the investigation of these splitting probabilities.

CHAPTER 4

MONTE CARLO SIMULATION OF POLYGON CONSTRUCTION

As we saw in Chapter 3, the expressions derived for the distributions of polygons in ρ^{**} are not manageable enough to obtain useful forms for the distributions of polygon characteristics of main interest namely N, S and A. In this chapter we demonstrate the real strength of the curling process, to efficiently select an independent and identically distributed sample of polygons from ρ^{**}.

4.1. Previous Studies.

Two previous Monte Carlo studies by Dufour [14] and Crain and Miles (1976) have been aimed at approximating the distributions of N, S and A in the isotropic case. Some of the estimates from these studies are presented in Tables 4.1 and 4.2 at the end of this section. In both of these studies, the simulation consisted of first simulating a Poisson field of lines in a fixed bounded region, and then extracting the polygons circumscribed by the lines in this region. For comparisons, we shall refer to this type of construction as the grouped method, and to the curling process construction as the sequential method.

In this section we discuss how several drawbacks of the grouped method are successfully avoided by the sequential method. We first compare speed and efficiency, and then examine some estimation issues. Crain and Miles also address these estimation issues and deal with them as effectively as possible within their constraints. They even point out how some of the stochastic constructions of polygons described in Miles (1973), which possess the independent identically distributed sampling properties of the sequential method, would avoid these problems.

First of all, the sequential method is substantially faster and requires far less computer memory than the grouped method. Dufour's analysis processes 947 polygons formed by 65 random lines. The information concerning Dufour's effort is unavailable, but the small number of polygons he analyzed suggests his methods were slow. The analysis by Crain and Miles processed 200,000 polygons in 66 sample discs. [15] They used about 15 hours of computer time on an IBM 360/50, a processing rate of about 200 per minute. They also required 180K bytes of memory just to store the information on each sampled disc. With the sequential method, we are able to process, in the isotropic case 2,500,000 polygons on a PDP 10/KI in just 4.76 hours, a rate of 8745 per minute. Furthermore, storage is minimal because polygons can be dispensed with as soon as they are processed. Adjusting these figures for the machine differences [16], we estimate that compared to the method of Crain and Miles our method is about 22 times faster while requiring virtually no storage. These differences in efficiency are probably due to the fact that the grouped method algorithms spend the bulk of their time searching for polygons, while the sequential method algorithms compute each polygon quickly as it is needed. It is interesting to note that Crain and Miles surmise that the stochastic constructions they suggest would require the same magnitude of computer effort per polygon as the grouped method.

The next comparisons concern estimation. The polygons generated by the grouped method are dependent in each region sampled. As a result, assessment of the precision of estimates is nontrivial since

the dependency is rather difficult to assess. The curling process on the other hand, by providing an i.i.d. sample, enables straightforward estimates of accuracy based on standard statistical methods. It can be argued that the grouped method provides more information such as estimates of the rate of ergodic convergence or the amount of dependency. Some of this information could be provided by the extensions of the curling process discussed in Section 3.7. However, due to the complexity of this type of information, we do not pursue it further.

Another problem that the grouped method must contend with is edge effects. That is, the boundary of the region sampled will necessarily intersect those polygons lying at the edge. The portions of these polygons lying outside the region are unobserved. To deal with this problem, one can undersample: exclude those polygons from the sample; or one can oversample: include those polygons together with estimates of their unseen properties. Crain and Miles use undersampling, and devise sophisticated techniques for weighting the sample to overcome bias (see Miles (1974)). There are no boundary constraints on the sequential method.

The last estimation issue we look at concerns the relationship of estimates to the intensity of the process. The grouped method essentially samples a Poisson field in a fixed bounded region as follows. First n, the number of hits, is selected from a Poisson distribution with intensity τ. Then n uniform random secants through this region are selected.

A subtle conceptual estimation problem is involved with this method. Namely, given n, the lines are more likely to come from a Poisson line process with the intensity of the maximum likelihood estimate of τ. The question then arises as for which intensity of a Poisson line process does the sampled region give the best estimates? This problem affects distributional estimates for S and A, whereas the distribution of N, as we showed in Section 3.2, is invariant under intensity changes. We do not face this problem with the sequential methods.

Probably because of the computer effort involved with the grouped method, previous Monte Carlo studies have focused exclusively on the case of most interest, isotropic ρ^{**}. The amount of extra computer effort required to extend the sequential method to the anisotropic case is small. The processing rate decreases to 5708 per minute in the slowest case we analyzed. The value of estimating the distributions of polygon characteristics in anisotropic ρ^{**} is that these distributions are the alternatives to isotropy which must be considered when devising statistical techniques for analysis.

TABLE 4.1

MONTE CARLO STUDY BY S. DUFOUR

ISOTROPIC POISSON FIELD — SAMPLE SIZE 947
INTENSITY τ=1

SAMPLE PERCENTILES

PROB(N = n)

n=	3	4	5	6	7
	.36	.38	.19	.054	.010

PROB(S < s)

s=	.5000	1.000	2.500	5.000
	.05	.11	.26	.51
s=	7.500	10.00	15.00	20.00
	.67	.79	.92	.98

PROB(A < a)

a=	.5000@-1	.1000	.2500	.5000	.7500
	.13	.18	.27	.38	.45
a=	1.000	2.500	5.000	10.00	15.00
	.50	.67	.80	.90	.95

TABLE 4.2

SOME MONTE CARLO ESTIMATES OF CRAIN AND MILES [16]

ISOTROPIC POISSON FIELD SAMPLE SIZE 200000

VARIOUS ESTIMATES OF
PROB(N = n)

n=	3	4	5	6	7
*STD	.3541	.3781	.1923	.0589	.0132
+STD	.3558	.3759	.1889	.06075	.01296
*WTD	.35561	.37790	.19183	.05922	.01318
+WTD	.35514	.37774	.18896	.6075	.01294
GRF	.355066	.381374	.189829	.058653	.012714
CRF	.355066	.379904	.190732	.059129	.012607

n=	8	9	10	11	12
*STD	.00188	.000262	.000015		
+STD	.00210	.000297	.000025	.0000032	.0000024
*WTD	.001958	.000248	.000038		
+WTD	.00208	.000291	.000024	.0000024	.0000025
GRF	.002071	.000265	.000027	.0000024	.00000017
CRF	.001958	.000230	.000021	.0000015	.000000086

4.2. Fast Simulation of $(Z_n,\Theta_{n+1})|\theta^{(n)}$.

(Note: We now drop the '~' notation for the curling process).

In this section we derive a simple and fast procedure for simulating the conditional random variables $Z_n|\theta^{(n)}$ and $\Theta_{n+1}|z^{(n)}$ in the curling process. This procedure is not only the basis for the efficiency of our simulation, but also lends substantial insight into the process of conditional hits in a Poisson field. To derive it from the curling process, we use the following theorem which shows quite clearly how linear Poisson processes of varying intensity arise from random censoring of linear Poisson processes of constant intensity.

Theorem 4.1.1. Let $\{W_i: i = 1,\ldots,\infty\}$ be a linear Poisson process on $(0,\infty)$ with constant intensity function ν. Let $q(w): (0,\infty) \to [0,1]$ be a measurable function. Let T_i, $i = 1,\ldots,\infty$ be random variables such that conditional on $W = (w_1,w_2,\ldots)$, the T_i are independent and

$$P\{(T_i|W) = 1\} = q(w_i) = 1 - P\{(T_i|W) = 0\} .$$

Define $S_1 = \inf\{i: T_i = 1\}$

and $S_n = \inf\{i: T_i = 1 \text{ and } i > S_{n-1}\}$.

Then

a) $dF_{W_{S_1}}(w) = \nu e^{-\nu Q(w)}\, q(w)dw$ where $Q(w) = \int_0^w q(w)dw$

b) $\{W_{S_i}; i=1,\ldots,\infty\}$ is a linear Poisson process with intensity function $\nu q(w)$.

Proof. (a) Let $E_n(w) = \{w_1,w_2,\ldots,w_n: 0 \le w_1 \le w_2 \le \cdots \le w_n \le w\}$

$$F_{W_{S_1}}(w) = \sum_{n=1}^{\infty} P\{S_1=n \text{ and } W_n \le w\}$$

$$= \sum_{n=1}^{\infty} \int_{E_n(w)} \prod_{i=1}^{n} \left[\nu e^{-\nu(w_i - w_{i-1})}(1-q(w_i))\right] \cdot \frac{q(w_n)}{1-q(w_n)}\, dw_1 dw_2 \cdots dw_n$$

where we define $w_0 \equiv 0$. By the Fubini theorem, we have

$$= \sum_{n=1}^{\infty} \int_0^w \nu e^{-\nu w_n} q(w_n) \left[\nu^{n-1} \int_{E_{n-1}(w_n)} \prod_{i=1}^{n-1} (1-q(w_i))dw_1 dw_2 \cdots dw_{n-1}\right] dw_n .$$

By symmetry,

$$= \sum_{n=1}^{\infty} \int_0^w \left[\nu e^{-\nu w_n} q(w_n) \frac{\nu^{n-1}}{(n-1)!} \cdot \int_{\substack{0 \le w_i \le w_n \\ i=1,\ldots,n-1}} \prod_{i=1}^{n-1} (1-q(w_i))dw_1 dw_2 \cdots dw_{n-1}\right] dw_n$$

Again using Fubini,

$$= \sum_{n=1}^{\infty} \int_0^w \nu e^{-\nu w_n} q(w_n) \left[\frac{\nu^{n-1}}{(n-1)!} \left| \int_0^{w_n} (1-q(w_1))dw_1 \right|^{n-1}\right] dw_n$$

$$= \sum_{n=1}^{\infty} \int_0^w \nu e^{-\nu w_n} q(w_n) \left[\frac{(\nu w_n - \nu Q(w_n))^{n-1}}{(n-1)!}\right] dw_n .$$

By monotone convergence (and replacing the dummy variable w_n by v for visual ease),

$$= \int_0^w \nu e^{-\nu v}\, q(v) \left[\sum_{n=0}^{\infty} \frac{(\nu v - \nu Q(v))^n}{n!} \right] dv$$

$$= \int_0^w \nu e^{-\nu v}\, q(v)\, e^{\nu v - \nu Q(v)}\, dv$$

$$= -e^{-\nu Q(v)} \Big|_0^w = 1 - e^{-\nu Q(w)} .$$

(a) follows by differentiating.

(c) By exploiting the independence of the W_i's (see (A.2)), and the conditional independence of the T_i's, the argument in (a) generalizes to yield the joint density for

$$W_{S(n)} = (W_{S_1}, \ldots, W_{S_n})$$

as

$$dF_{W_{S(n)}}(w_{S(n)}) = \nu^n \Big(\prod_{i=1}^{n} q(w_{S_i}) \Big)\, e^{-\nu Q(w_{S_n})}\, dw_{S(n)}$$

the desired joint density. ||

Now recall that the conditional density of $(Z_n | \theta^{(n)})$, (side length in the curling process), was derived in Section 2.6, (2.23), as

$$dF_{Z_n | \theta^{(n)}}(z_n) = \tau q(z_n, \theta^{(n)}) \exp\{-\tau Q(z_n, \theta^{(n)})\} dz_n \qquad (4.1)$$

where $q(z_n,\theta^{(n)})$ and $Q(z_n,\theta^{(n)})$ are defined in (2.13) and (2.24) respectively. Referring to Figure 3.1, intuitively z_n is the distance from v_n along ℓ_n to v_{n+1} given that ℓ_{n+1} does not cross back through the polygon being formed.

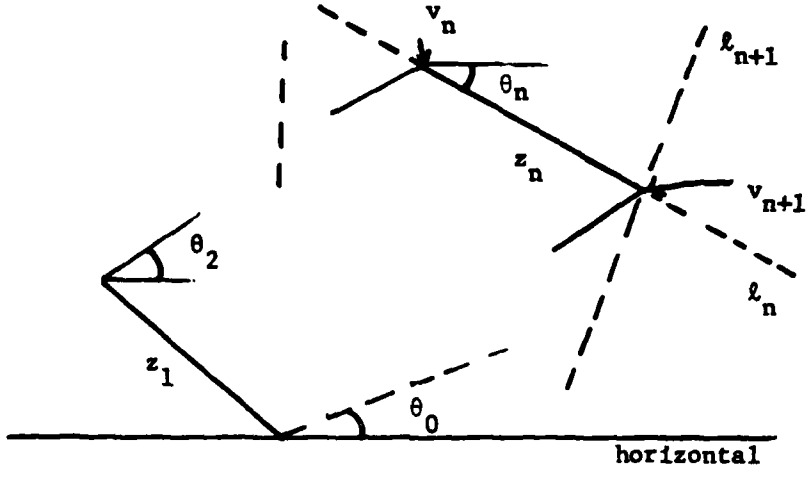

Figure 3.1.

We make the following identifications with Theorem 4.1.1. Let $\{W_i\}$ correspond to the point process of hits along ℓ_n starting from v_n unconditionally, i.e. as if ℓ_n were an arbitrary line in $\mathcal{L}$. By Theorem 1.2.2, $\{W_i\}$ is a linear Poisson point process with constant intensity

$$\nu = \tau\lambda(\theta_n) \quad . \tag{4.2}$$

Associate with each point W_i the angle Φ_i that ℓ_n makes with the intersecting line. The angles Φ_i are i.i.d. with the density

$$(4.3) \qquad dF(\phi_i) = (\lambda(\theta_n))^{-1} \sin(\theta_n - \phi) dG(\phi) \quad \text{for } \phi \in (\theta_n - \pi, \theta_n)$$

given by (1.22) from Theorem 1.2.3. From Section 2.5, ϕ_i would be a 'legal' candidate for θ_{n+1} if $\phi_i \in (\alpha_i, \theta_n)$ where α_i corresponds to the angle of the diagonal from v_1 to w_i as in (2.11) and (2.14).

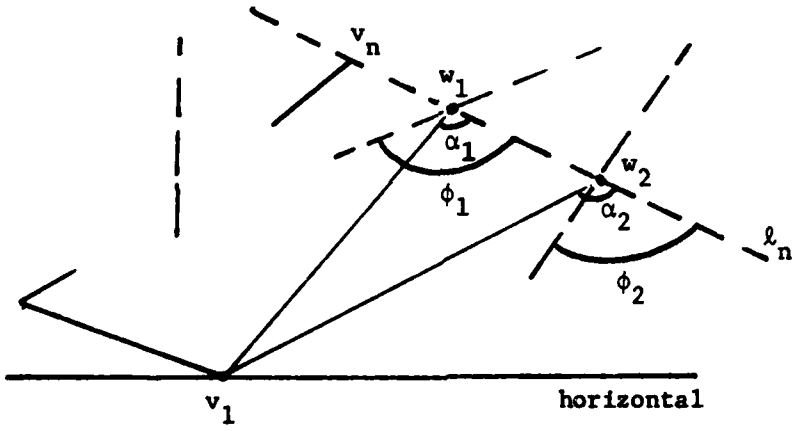

Figure 3.2.

For example in Figure 3.2, ϕ_1 is not 'legal' but ϕ_2 is.

Define

$$T_i = \begin{cases} 1 & \text{if } \phi_i \in (\alpha_i, \theta_n) \\ 0 & \text{if } \phi_i \notin (\alpha_i, \theta_n) . \end{cases}$$

Then from (4.3) and (2.13), $P\{T_i|W\} = q(w_i)$ where

$$q(w_i) = \lambda(\theta_n)^{-1} \int_{(\alpha_i,\theta_n)} dF(\phi_i) \tag{4.4}$$

$$= \frac{q(w,\theta^{(n)})}{\lambda(\theta_n)} .$$

Combining (4.2) and (4.4) with Theorem 4.1.1(a), we observe that

$$dF_{W_{S_1}}(w) = \nu \exp\{-\nu Q(w)\}q(w)dw \tag{4.5}$$

$$= \tau q(w,\theta^{(n)})\exp\{-\tau Q(w,\theta^{(n)})\}dw$$

which is precisely the same density as $dF_{Z_n|\theta^{(n)}}$ in (4.1). Furthermore, the independence of the Φ_i's allows us to infer that

$$dF_{\Phi_{S_1}|w_{s_1}}(\phi) = ((q(w_{s_1},\theta^{(n)}))^{-1} \sin(\theta_n-\phi)dG(\phi) \tag{4.6}$$

for $\phi \in (\alpha_{s_1},\theta_n)$, precisely the density $dF_{\theta_{n+1}|z^{(n)}}$ given by (2.12).

We summarize the above results in the following theorem.

Theorem 4.1.2. Let $V_1, V_2, \ldots$ be i.i.d. with exponential density

$$dF(v) = \tau\lambda(\theta_n)\exp\{-\tau\lambda(\theta_n)v\}dv \ , \quad v \in (0,\infty) \ . \tag{4.7}$$

Let $\Phi_1, \Phi_2, \ldots$ be i.i.d. (and independent of the V_i's) with density

$$dF(\phi) = (\lambda(\theta_n))^{-1} \sin(\theta_n - \phi)dG(\phi) \ , \quad \phi \in (\theta_n - \pi, \theta_n) \ . \tag{4.8}$$

Let

$$T = \inf\{i: \phi \in (\alpha_i, \theta_n)\}.$$

Then $Z_n = \sum_{i=1}^{T} V_i$ and $\Theta_{n+1} = \Phi_T$ have the bivariate conditional density

$$dF_{Z_n, \Theta_{n+1} | \theta^{(n)}}(z_n, \theta_{n+1}) = \tau \sin(\theta_n - \theta_{n+1}) \cdot \exp\{-\tau Q(z_n, \theta^{(n)})\} \, dG(\theta_{n+1})dz_n \tag{4.9}$$

on $z_n \in (0,\infty)$, $\theta_{n+1} \in (\alpha_n, \theta_n)$.

(Note that the joint density appearing in (4.9) is obtained as the product of (2.12) and (2.22)).

In the following flow diagram we illustrate the ease with which Theorem 4.1.2 enables us to simulate Z_n and Θ_{n+1}. The particular techniques for simulating V_i and Φ_i in the middle steps are discussed in the next section.

Procedure for Generating Z_n, θ_{n+1} from $dF_{Z_n,\theta_{n+1}|\theta^{(n)}}$

(4.10)

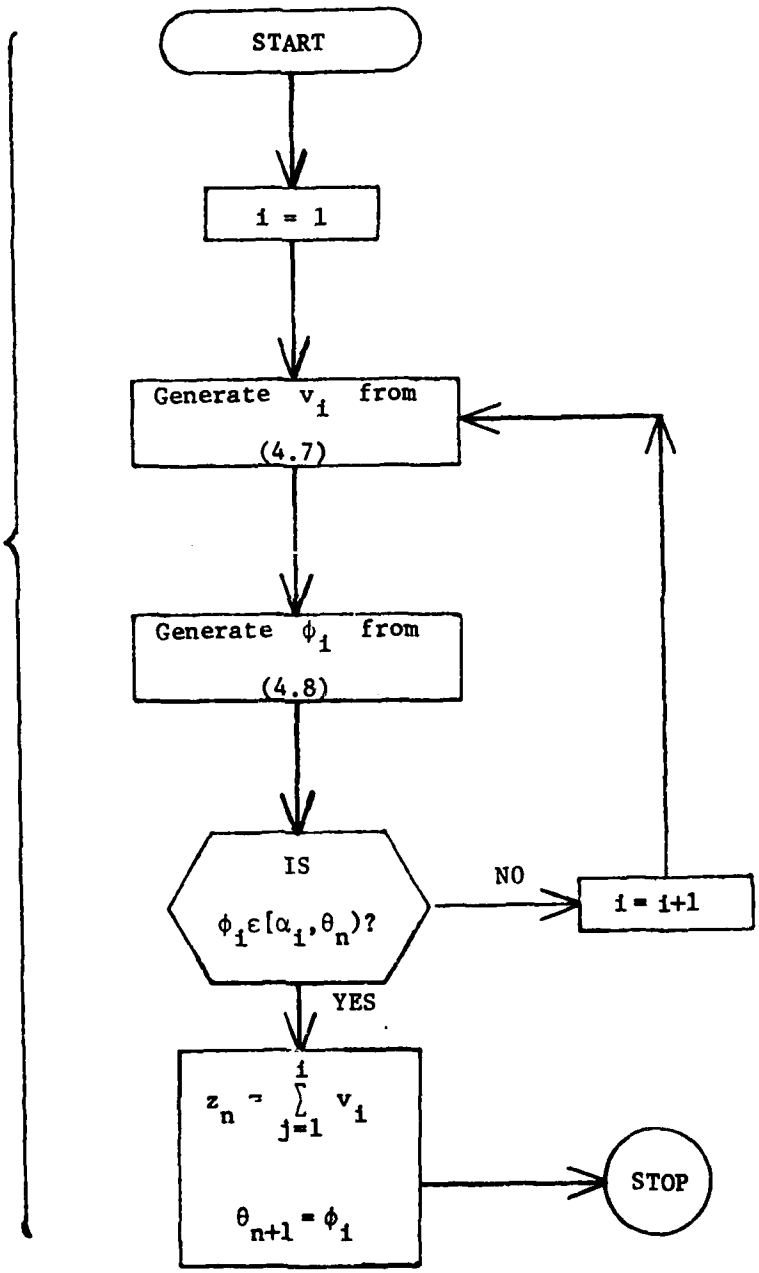

We remark that a particularly nice programming feature of the procedure (4.10) is that we require only x_{n-1}, y_{n-1}, (see (2.5)), and θ_n from $\theta^{(n)}$ for the calculation of $\lambda(\theta_n)$ and the bounds (α_i, θ_n), (see (2.14)). As discussed in Section 4.4, this information is easily and necessarily stored sequentially during execution of the main program.

4.3. Some Simulation Techniques.

Our computer system provides, as do most computer systems, a fast routine for generating an independent sequence of uniform [0,1] random variables, which we shall denote by $\xi_1, \xi_2, \ldots$. [17] To generate a general independent sequence of random variables $\eta_1, \eta_2, \ldots$ with distribution function F, it is well known that we can simply take $\eta_i = F^{-1}(\xi_i)$. How well this works in practice depends on the ease with which we can invert F.

To generate V_i in (4.10) we simply take $V_i = (\tau\lambda(\theta_n))^{-1} \log \xi_i$ as the exponential distribution (4.7) is easy to invert. The difficulty of simulating $Z_n | \theta^{(n)}$ directly from the distribution induced by the density (2.18) should be apparent. Inevitably it would require evaluation of $\Lambda^{-1}(\xi)$ where $\Lambda(z_n) = \frac{\tau}{2} [z\lambda(\theta_n) + d_n\lambda(\alpha_n) - d_{n-1}\lambda(\alpha_{n-1})]$, a calculation hopeless by analytical methods and very long by numerical methods.

The generation of Φ_i in (4.10) takes a bit more doing. Although in the isotropic case the distribution (4.8) is easy to invert, in the anisotropic case this is not generally true. To get around this problem, we resort to an old-fashioned simulation method, the general rejection technique. An informative discussion of this technique, apparently introduced by von Neumann, appears in Butler (1956).

We describe our application of the rejection technique to the simulation of Φ_i with the flow diagram below. We first need the following notation. Rewrite the density (4.8) of Φ_i as

(4.11) $$dF(\phi) = K\, g(\phi)\, dH(\phi)$$

where $g(\phi)d\phi = dG(\phi)$, $dH(\phi) = \frac{1}{2}\sin(\theta_n - \phi)d\phi$ and K is a normalizing constant. Let $m > 0$ be such that $m \sup_{\phi} g(\phi) \leq 1$, (preferably = for maximum efficiency).

Notice that H is easily invertible as $H(\xi) = \arccos(1-2\xi) + \theta_n - \pi$ for $\xi \in [0,1]$.

Procedure for Generating Φ_1 from $dF(\phi)$ in (4.8).

(4.12)

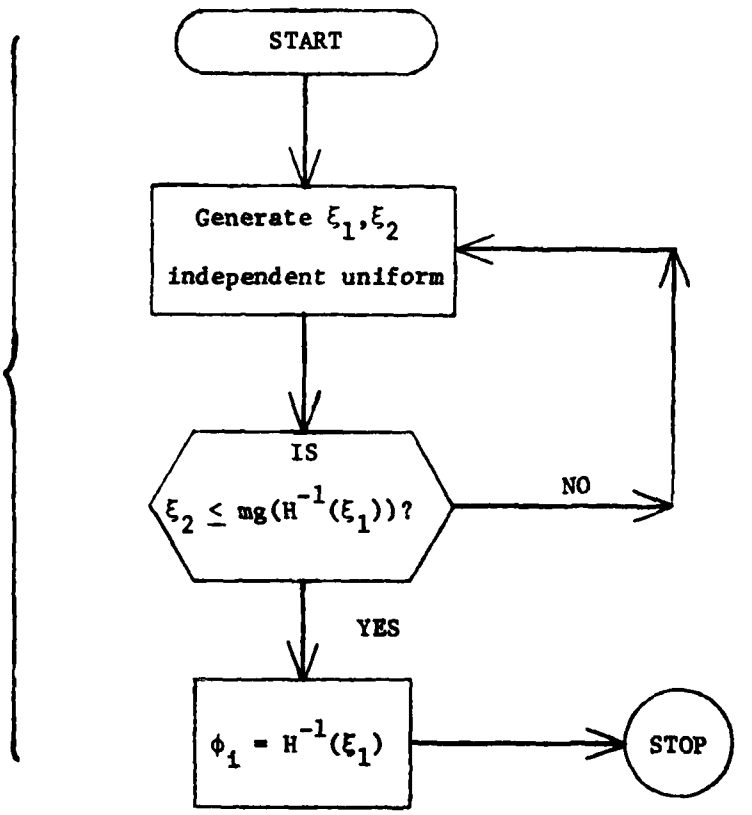

This technique seems to work quite well as long as $g = dG$ is not too variable. However, if it is very variable and G^{-1} is readily obtainable, we can reverse the roles of H and G in (4.9) to achieve greater efficiency.

To show that the density of the ϕ_i generated by (4.12) is correct simply notice that

$$P\{\xi_2 < mg(H^{-1}(\xi_1))|\xi_1\} \propto g(H^{-1}(\xi_1)) .$$

Since ξ_1 is uniform on $[0,1]$, the density of $\phi_i = H^{-1}(\xi_1)$ is

$$dF(\phi) \propto g(\phi)\, dH(\phi)$$

agreeing with (4.11).

We use the same general ideas for generating θ_0 and θ_1 from the joint density dF_{θ_0,θ_1} appearing in (2.7). First we generate η_0 with density dG, by taking $G^{-1}(\xi)$ if G^{-1} is easily obtainable, or by (4.12) with $dH \equiv 1$. Then we generate η_1 by (4.12) with $H^{-1}(\xi) = \arccos(1-2\xi) + \eta_0$. Finally, we obtain $\theta_0 = \min(\eta_0,\eta_1)$ and $\theta_1 = \max(\eta_0,\eta_1)$.

4.4. The Simulated Curling Process.

We present in this section the flow diagram outlining the programming steps for the generation of each random polygon by the curling process. The steps at which θ_0, θ_1 and (z_n, θ_{n+1}) are generated, incorporate the methods developed in Sections 4.2 and 4.3. We implement these methods as subroutines in our program.

As each polygon is generated we need to output N, S and A for computing the statistics we tabulate. Each of these polygon characteristics can be obtained by incrementing partial sums as each side length and angle (z_n, θ_{n+1}) is generated. In the flow diagram we will use the following notation for formulas required to compute and save partial information during execution. This notation corresponds to (2.4), (2.5), (2.6), (3.1) and (3.3) which are necessary for the calculation of N, S and A.

$$
(4.13)\quad \begin{cases} x_n = \sum_{i=1}^{n} z_i \cos \theta_i \\ y_n = \sum_{i=1}^{n} z_i \sin \theta_i \\ u_n = -\sec(\theta_n - \theta_0) \sum_{i=1}^{n-1} z_i \sin(\theta_i - \theta_0) \\ s_n = \sum_{i=1}^{n} z_n \\ a_n = \frac{1}{2} \sum_{i=1}^{n} (x_i - x_{i-1})(y_i + y_{i-1}) , \qquad (x_0, y_0) \equiv (0,0) . \end{cases}
$$

In the last branch of the construction, after N has been obtained, we compute z_{N-1}, θ_N and z_N from (4.13) via (2.3) as

$$z_{N-1} = - u_{N-1}$$

$$\theta_N = \theta_0 - \pi$$

$$z_N = (x_{N-1}^2 + y_{N-1}^2)^{1/2}$$

Flow Diagram for Curling Process Construction

of Random Polygons

(4.14)

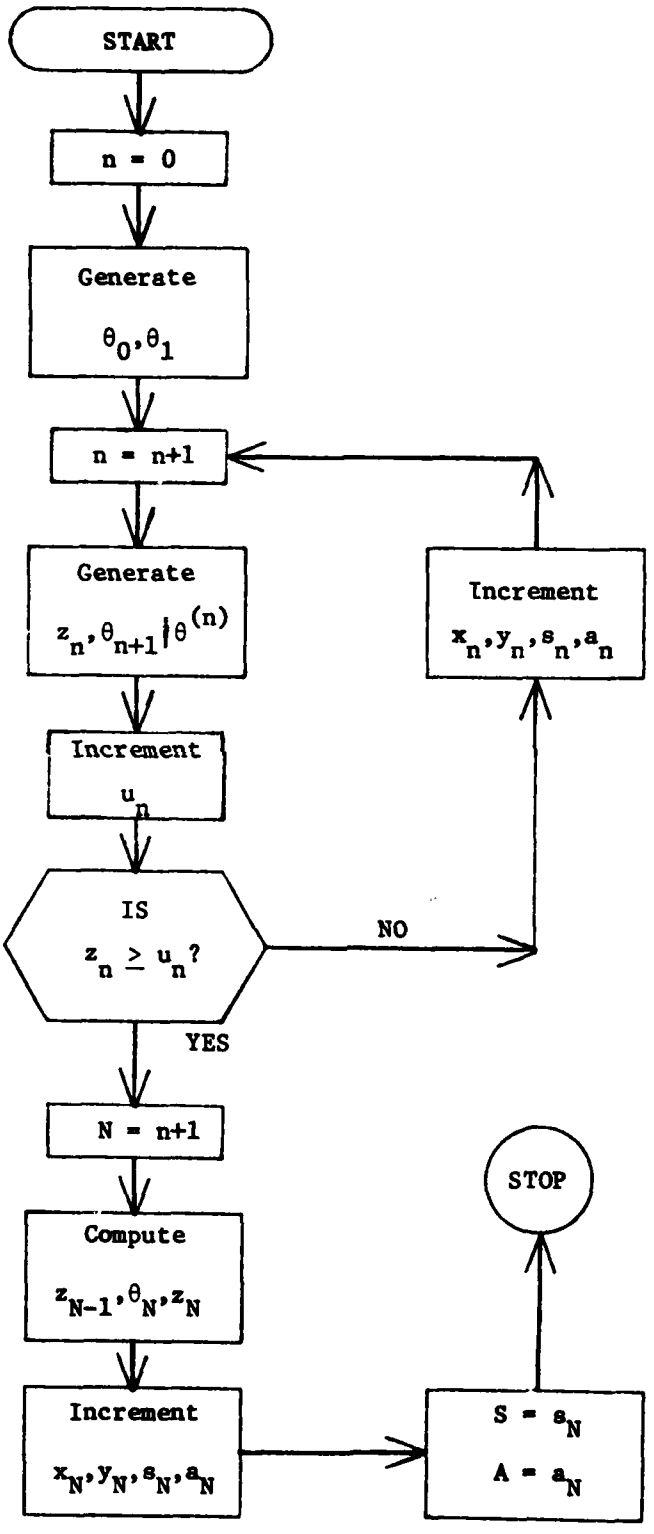

4.5. Simulation Results.

In this final section the results of a Monte Carlo investigation of the distributions of N, S, and A in various ρ^* by simulation of the curling process, are presented in three subsections consisting of the isotropic case, some anisotropic cases induced by members of φ^C, and some anisotropic cases induced by members of φ^D. The intensity of the Poisson field is kept at $\tau = 1$ in all the simulations. The related distributions for different intensities follow immediately from the observations made at the end of Sections 3.2 and 3.3.

Three tables are presented for each case. The first table presents sample percentiles. The second presents sample moments, the estimated standard error of the estimates, and the numerical values for some of the known moments given in (3.20) and (3.38). These are provided for an assessment of the numerical accuracy of our computing facilities. The last table lists characteristics of the twenty five largest polygons (in area) sampled. Included in this list is the isoperimetric ratio $I = S^2/4\pi A$ for each of these polygons. The well known isoperimetric inequality states that $I \geq 1$, with equality holding only for a circle. Thus I is a measure of the circularity of a polygon.

4.5.1. The Isotropic Case.

Tables 4.3a-c present the results for the isotropic case. Being the case of primary interest in the literature, a sample size of 2,500,000 polygons was simulated with the goal of obtaining the most precise estimates of the unknown distributional characteristics to date. Fortunately,

the simulation rate of 8745 polygons per minute, was the fastest of the simulations. This was probably due to the fact that angle simulation here did not require the somewhat inefficient rejection technique discussed in Section 4.3.

The width of the 99% confidence band about the sample distribution function induced by the percentile estimates in Table 4.3a is obtained from the familiar Kolmogorov statistic as .00103. (Hence the band for the N probabilities given is .00206). The estimates for N provided by Dufour, and Crain and Miles in Tables 4.1 and 4.2 are close but not always within these limits. It is comforting to compare the estimate .3552 of $P\{N=3\}$ with the known theoretical value of .3551 derived in (3.27).

The sample moments presented in Table 4.3b seem to be extraodinarily accurate. Indeed, the estimates of the known moments are in every case within half of a standard error of the true value! Thus, there is every reason to believe that the estimates of the unknown moments are similarly accurate and can perhaps be useful in the pursuit of the theoretical values.

The largest polygons (in area) sampled are listed in Table 4.3c. The initial motivation for providing this list of extreme values was to investigate a conjecture by D.G. Kendall [19] that $I|A \to 1$ as $A \to \infty$, that the largest polygons in area tend to be circular. The isoperimetric ratios in the table do not appear to be getting smaller though it is perhaps unreasonable to expect that this sample size emulates what happens near infinity. What this facinating conjecture does bring to mind however, is whether or not the large polygons are

many sided. It is interesting to note that of the 53 polygons with 10 or more sides in the sample, none appeared in this list. Finally, if ıdall's conjecture is false, the next question to ask is, to what value does $I|A$ converge as $A \to \infty$ if it converges at all?

TABLE 4.3a

ISOTROPIC CASE
$G_{(0)}$

SAMPLE SIZE 2500000
PROCESSING RATE 8745/MIN

SAMPLE PERCENTILES

PROB(N = n)

n=	3	4	5	6	7
	.3552	.3814	.1895	.5870@-1	.1275@-1
n=	8	9	10	11	12
	.2082@-2	.2712@-3	.1800@-4	.2800@-5	.4000@-6

(0 POLYGONS WITH N > 12)

PROB(S < s)

s=	.1000	.2500	.5000	.7500	1.000
	.1128@-1	.2842@-1	.5699@-1	.8528@-1	.1135
s=	1.500	2.500	3.750	5.000	6.250
	.1693	.2764	.3995	.5080	.6013
s=	7.500	8.750	10.00	12.50	15.00
	.6801	.7455	.7987	.8765	.9257
s=	17.50	20.00	25.00	30.00	50.00
	.9561	.9744	.9917	.9974	1.000

(54 POLYGONS WITH S > 50)

PROB(A < a)

a=	.5000@-2	.1000@-1	.2500@-1	.5000@-1	.1000
	.4536@-1	.6388@-1	.9968@-1	.1392	.1931
a=	.2500	5000	.7500	1.000	1.500
	.2924	.3926	.4615	.5140	.5929
a=	2.500	5.000	7.500	10.00	12.50
	.6944	.8228	.8846	.9201	.9424
a=	15.00	20.00	30.00	50.00	100.0
	.9574	.9752	.9902	.9978	.9999

(334 POLYGONS WITH A > 100)

TABLE 4.3b

ISOTROPIC CASE
$G_{(0)}$

SAMPLE SIZE 2500000
PROCESSING RATE 8745/MIN

SAMPLE MOMENTS

		N	S	A
1ST MOMENT	=	3.99980	6.28409	3.14061
(STD ERR)		.6116@-3	.3401@-2	.3934@-2
2ND MOMENT	=	16.9336	68.4150	48.5634
(STD ERR)		.5490@-2	.7704@-1	.2052
3RD MOMENT	=	76.0337	1028.67	1718.34
(STD ERR)		.3977@-1	2.073	23.32
4TH MOMENT	=	362.110	19520.2	107669.
(STD ERR)		.2768	68.18	4225.
5TH MOMENT	=	1826.58	444941.	.103294@8
(STD ERR)		1.954	2665.	.9695@6
6TH MOMENT	=	9735.80	.118016@8	.136291@10
(STD ERR)		14.32	.1192@6	.2483@9

KNOWN MOMENTS

		N	S	A
1ST MOMENT	=	4.00000	6.28319	3.14159
2ND MOMENT	=	16.9356	68.4438	48.7045
3RD MOMENT	=	unknown	unknown	1725.88

TABLE 4.3c

ISOTROPIC CASE
$G_{(0)}$

SAMPLE SIZE 2500000
PROCESSING RATE 8745/MIN

THE 25 LARGEST POLYGONS (IN AREA)
I =ISOPERIMETRIC RATIO

RANK	N	S	A	I
1	8.000	64.71	285.0	1.169
2	6.000	61.95	243.8	1.252
3	9.000	59.18	219.1	1.272
4	7.000	55.94	206.1	1.208
5	6.000	54.77	203.0	1.176
6	6.000	57.20	199.3	1.306
7	8.000	55.2[illegible]	193.4	1.255
8	8.000	54.20	192.8	1.212
9	6.000	57.89	187.6	1.421
10	7.000	51.27	185.8	1.126
11	8.000	53.92	184.6	1.253
12	9.000	53.65	181.2	1.264
13	9.000	50.17	180.3	1.111
14	6.000	62.70	177.4	1.763
15	6.000	52.98	172.2	1.297
16	6.000	58.73	171.2	1.603
17	7.000	50.21	170.8	1.174
18	9.000	53.00	169.4	1.319
19	8.000	50.50	168.4	1.205
20	8.000	52.30	166.7	1.306
21	7.000	53.74	165.8	1.386
22	8.000	53.02	165.2	1.354
23	7.000	48.07	163.9	1.122
24	7.000	54.43	160.9	1.465
25	5.000	49.71	159.0	1.237

AD-A119 410 STANFORD UNIV CA DEPT OF STATISTICS F/G 12/1
SEQUENTIAL STOCHASTIC CONSTRUCTION OF RANDOM POLYGONS.(U)
JUN 82 E I GEORGE N00014-76-C-0475
UNCLASSIFIED TR-320 NL

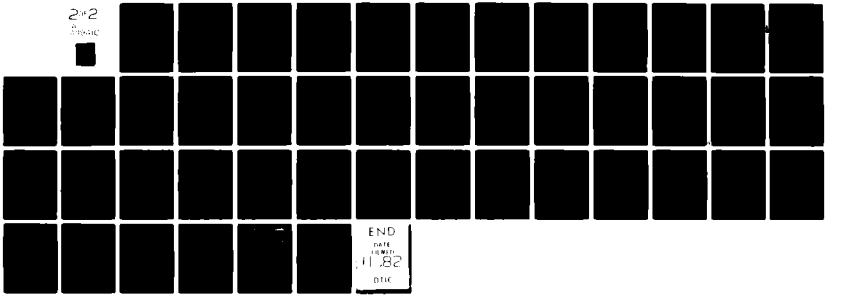

4.5.2. Anisotropic Cases Induced by $\mathcal{G}^C$.

Tables 4.4a through 4.7c present the simulation results for anisotropic cases induced by the following four members of $\mathcal{G}^C$.

$$dG_{(2,0,1,1,\pi/2,0,0)}(\theta) = (2\pi)^{-1}(1 + \frac{\pi}{2}\sin\theta)d\theta$$

$$dG_{(2,0,2,1,2,0,0)}(\theta) = (2\pi)^{-1}(1 + 2\sin^2\theta)d\theta$$

$$dG_{(2,0,4,1,8/3,0,0)}(\theta) = (2\pi)^{-1}(1 + (8/3)\sin^4\theta)d\theta$$

$$dG_{(2,4,4,1,1,0,\pi/3)}(\theta) = \frac{16}{3\pi}(\sin^4\theta + \sin^4(\theta - \frac{\pi}{3}))\,d\theta$$

The first three distributions are mixtures of the uniform with progressively sharper pulses. In each case the pulses are weighted so as to contribute half of the total probability to the mixture. The last case is a mixture of two sharp pulses located at a distance of $\pi/3$ from each other. The functions $\lambda(\theta)$ for each of the distributions are obtained from (1.20) and (3.37)-(3.40).

The purpose of these simulations was exploratory so that sample sizes were kept to 100,000, far smaller than the 2,500,000 for the isotropic case. The simulation rate for the first case was 7211 polygons per minute and decreased to 5708 per minute in the last case. Ostensibly, this decreasing rate was primarily due to increased inefficiency of the rejection technique for simulating the angle distribution with sharper pulses. Nonetheless, this slowest case is still quite fast as it took only a total of 17.52 minutes of cpu time.

Turning immediately to the tables of sample moments in each of these cases, we see that the accuracy of the simulation is breaking

down. For example, estimates of E[N] are underestimated by several standard errors in every case. Extensive investigation into this discrepancy revealed that the problem is due to numerical rounding error which accumulates in the less stable anisotropic cases. Correction of this inaccuracy would require the use of a more accurate programming language. [20]

In light of these numerical problems, the high precision from our sample size is irrelevant. Nonetheless, the estimates themselves are close enough to the true values so that general information about the nature of the distributions of N, S, and A in these anisotropic cases can be gleaned from the results. Also, the inaccuracies are less severe for the estimates with S and A. Rather than go into a lengthy analysis of these results, we observe that none of these cases differ markedly from the isotropic case.

TABLE 4.4a

ANISOTROPIC CASE
$G_{(2,0,1,1,\pi/2,0,0)}$

SAMPLE SIZE 100000
PROCESSING RATE 7211/MIN

SAMPLE PERCENTILES

PROB(N = n)

n=	3	4	5	6	7
	.3580	.3815	.1892	.5661@-1	.1224@-1
n=	8	9	10	11	12
	.2050@-2	.3300@-3	.5000@-4	.0000	.0000

(0 POLYGONS WITH N > 12)

PROB(S < s)

s=	.1000	.2500	.5000	.7500	1.000
	.1069@-1	.2706@-1	.5516@-1	.8378@-1	.1122
s=	1.500	2.500	3.750	5.000	6.250
	.1668	.2734	.3943	.5018	.5944
s=	7.500	8.750	10.00	12.50	15.00
	.6731	.7394	.7930	.8714	.9225
s=	17.50	20.00	25.00	30.00	50.00
	.9534	.9728	.9907	.9971	1.000

(4 POLYGONS WITH S > 50)

PROB(A < a)

a=	.5000@-2	.1000@-1	.2500@-1	.5000@-1	.1000
	.4376@-1	.6269@-1	.9958@-1	.1389	.1920
a=	.2500	.5000	.7500	1.000	1.500
	.2900	.3902	.4589	.5115	.5903
a=	2.500	5.000	7.500	10.00	12.50
	.6919	.8208	.8832	.9192	.9416
a=	15.00	20.00	30.00	50.00	100.0
	.9566	.9746	.9901	.9978	.9999

(15 POLYGONS WITH A > 100)

TABLE 4.4b

ANISOTROPIC CASE
$G_{(2,0,1,1,\pi/2,0,0)}$

SAMPLE SIZE 100000
PROCESSING RATE 7211/MIN

SAMPLE MOMENTS

		N	S	A
1ST MOMENT	=	3.99135	6.38409	3.17273
(STD ERR)		.3044@-2	.1729@-1	.1986@-1
2ND MOMENT	=	16.8574	70.6676	49.5250
(STD ERR)		.2731@-1	.4007	1.079
3RD MOMENT	=	75.5022	1082.84	1796.20
(STD ERR)		.1981	11.24	127.0
4TH MOMENT	=	358.748	21048.0	118871.
(STD ERR)		1.385	398.9	.206@@5
5TH MOMENT	=	1806.57	496054.	.12102@@8
(STD ERR)		9.868	.173@@5	.374@@7
6TH MOMENT	=	9624.29	.13800@@8	.161634@10
(STD ERR)		73.27	.875@@6	.708@@9

KNOWN MOMENTS

		N	S	A
1TH MOMENT	=	4.00000	6.40278	3.20139
2TH MOMENT	=	16.9330	unknown	50.5583

TABLE 4.4c

ANISOTROPIC CASE
$G_{(2,0,1,1,\pi/2,0,0)}$

SAMPLE SIZE 100000
PROCESSING RATE 7211/MIN

THE 25 LARGEST POLYGONS (IN AREA)
I =ISOPERIMETRIC RATIO

RANK	N	S	A	I
1	6.000	55.86	199.8	1.242
2	7.000	52.38	167.1	1.306
3	4.000	52.74	163.7	1.352
4	6.000	45.74	134.6	1.237
5	7.000	47.20	128.6	1.378
6	6.000	45.62	125.7	1.317
7	6.000	45.78	121.4	1.373
8	7.000	42.63	120.3	1.202
9	8.000	39.86	115.8	1.092
10	7.000	42.59	111.2	1.298
11	6.000	45.60	109.8	1.508
12	8.000	42.38	105.6	1.354
13	7.000	48.99	104.9	1.821
14	7.000	42.99	103.5	1.421
15	6.000	41.18	102.0	1.323
16	6.000	62.47	98.57	3.151
17	9.000	37.07	97.13	1.126
18	6.000	39.39	95.57	1.292
19	8.000	40.67	95.01	1.385
20	5.000	40.14	91.83	1.396
21	7.000	36.87	90.47	1.196
22	8.000	40.37	89.26	1.453
23	6.000	37.00	87.25	1.249
24	7.000	42.20	86.17	1.645
25	6.000	47.24	86.09	2.063

TABLE 4.5a

ANISOTROPIC CASE
$G_{(2,0,2,1,2,0,0)}$

SAMPLE SIZE 100000
PROCESSING RATE 7159/MIN

SAMPLE PERCENTILES

PROB(N = n)

n=	3	4	5	6	7
	.3603	.3810	.1877	.5675E-1	.1215E-1
n=	8	9	10	11	12
	.1750E-2	.3500E-3	.3000E-4	.0000	.0000

(0 POLYGONS WITH N > 12)

PROB(S < s)

s=	.1000	.2500	.5000	.7500	1.000
	.1072E-1	.2683E-1	.5503E-1	.8327E-1	.1106
s=	1.500	2.500	3.750	5.000	6.250
	.1666	.2716	.3914	.4957	.5881
s=	7.500	8.750	10.00	12.50	15.00
	.6661	.7306	.7853	.8656	.9173
s=	17.50	20.00	25.00	30.00	50.00
	.9498	.9704	.9897	.9962	1.000

(4 POLYGONS WITH S > 50)

PROB(A < a)

a=	.5000E-2	.1000E-1	.2500E-1	.5000E-1	.1000
	.4454E-1	.6308E-1	.9850E-1	.1384	.1928
a=	.2500	.5000	.7500	1.000	1.500
	.2922	.3910	.4590	.5111	.5890
a=	2.500	5.000	7.500	10.00	12.50
	.6904	.8192	.8823	.9182	.9406
a=	15.00	20.00	30.00	50.00	100.0
	.9564	.9744	.9900	.9975	.9999

(14 POLYGONS WITH A > 100)

TABLE 4.5b

ANISOTROPIC CASE
$G_{(2,0,2,1,2,0,0)}$

SAMPLE SIZE 100000
PROCESSING RATE 7159/MIN

SAMPLE MOMENTS

		N	S	A
1ST MOMENT	=	3.98629	6.49553	3.19942
(STD ERR)		.3036E-2	.1773E-1	.2016E-1
2ND MOMENT	=	16.8125	73.6189	50.8863
(STD ERR)		.2718E-1	.4229	1.103
3RD MOMENT	=	75.1797	1160.47	1890.60
(STD ERR)		.1964	12.22	121.8
4TH MOMENT	=	356.511	23306.9	124244.
(STD ERR)		1.365	438.4	.185E5
5TH MOMENT	=	1790.74	568391.	.11996E8
(STD ERR)		9.649	.188E5	.321E7
6TH MOMENT	=	9507.88	.16290E8	.14881E10
(STD ERR)		70.91	.929E6	.584E9

KNOWN MOMENTS

		N	S	A
1TH MOMENT	=	4.00000	6.55637	3.27819
2TH MOMENT	=	16.9333	unknown	53.0157

TABLE 4.5c

ANISOTROPIC CASE
$G_{(2,0,2,1,2,0,0)}$

SAMPLE SIZE 100000
PROCESSING RATE 7159/MIN

THE 25 LARGEST POLYGONS (IN AREA)
I =ISOPERIMETRIC RATIO

RANK	N	S	A	I
1	8.000	61.59	193.9	1.557
2	8.000	46.90	154.7	1.132
3	6.000	59.65	153.7	1.843
4	7.000	51.00	149.9	1.381
5	7.000	49.39	142.3	1.364
6	7.000	43.06	120.5	1.224
7	5.000	47.54	113.2	1.589
8	5.000	43.01	108.0	1.363
9	6.000	43.95	107.5	1.431
10	7.000	42.34	104.8	1.361
11	6.000	40.12	103.8	1.233
12	7.000	51.58	101.5	2.087
13	6.000	40.54	101.1	1.294
14	4.000	41.49	101.0	1.356
15	8.000	40.49	98.96	1.318
16	6.000	39.35	98.32	1.254
17	7.000	40.39	97.79	1.328
18	7.000	44.18	97.39	1.595
19	6.000	41.04	97.09	1.381
20	5.000	41.75	96.35	1.440
21	8.000	41.41	96.30	1.417
22	5.000	42.48	96.24	1.492
23	6.000	40.90	95.34	1.396
24	4.000	43.94	95.02	1.617
25	7.000	38.01	94.96	1.211

TABLE 4.6a

ANISOTROPIC CASE
$G_{(2,0,4,1,8/3,0,0)}$

SAMPLE SIZE 100000
PROCESSING RATE 6282/MIN

SAMPLE PERCENTILES

PROB(N = n)

n=	3	4	5	6	7
	.3635	.3834	.1836	.5612@-1	.1143@-1
n=	8	9	10	11	12
	.1780@-2	.1500@-3	.2000@-4	.1000@-4	.0000

(0 POLYGONS WITH N > 12)

PROB(S < s)

s=	.1000	.2500	.5000	.7500	1.000
	.1066@-1	.2725@-1	.5422@-1	.8084@-1	.1078
s=	1.500	2.500	3.750	5.000	6.250
	.1619	.2633	.3820	.4865	.5743
s=	7.500	8.750	10.00	12.50	15.00
	.6521	.7179	.7734	.8545	.9079
s=	17.50	20.00	25.00	30.00	50.00
	.9422	.9645	.9870	.9951	1.000

(4 POLYGONS WITH S > 50)

PROB(A < a)

a=	.5000@-2	.1000@-1	.2500@-1	.5000@-1	.1000
	.4443@-1	.6308@-1	.9824@-1	.1373	.1908
a=	.2500	.5000	.7500	1.000	1.500
	.2889	.3897	.4561	.5082	.5860
a=	2.500	5.000	7.500	10.00	12.50
	.6862	.8154	.8785	.9149	.9373
a=	15.00	20.00	30.00	50.00	100.0
	.9532	.9726	.9889	.9972	.9999

(15 POLYGONS WITH A > 100)

TABLE 4.6b

ANISOTROPIC CASE
$G_{(2,0,4,1,8/3,0,0)}$

SAMPLE SIZE 100000
PROCESSING RATE 6282/MIN

SAMPLE MOMENTS

		N	S	A
1ST MOMENT	=	3.97474	6.72080	3.29444
(STD ERR)		.3012@-2	.1848@-1	.2069@-1
2ND MOMENT	=	16.7058	79.3305	53.6550
(STD ERR)		.2685@-1	.4602	1.061
3RD MOMENT	=	74.4005	1307.63	1944.86
(STD ERR)		.1928	13.78	95.11
4TH MOMENT	=	351.152	27472.4	115541.
(STD ERR)		1.329	500.0	.1087@5
5TH MOMENT	=	1754.04	698314.	.932241@7
(STD ERR)		9.304	.2092@5	.1388@7
6TH MOMENT	=	9251.63	.20698l@8	.90831O@9
(STD ERR)		67.99	.9654@6	.1882@9

KNOWN MOMENTS

		N	S	A
1TH MOMENT	=	4.00000	6.79264	3.39632
2TH MOMENT	=	16.9346	unknown	56.9205

TABLE 4.6c

ANISOTROPIC CASE
$G_{(2,0,4,1,8/3,0,0)}$

SAMPLE SIZE 100000
PROCESSING RATE 6282/MIN

THE 25 LARGEST POLYGONS (IN AREA)
I =ISOPERIMETRIC RATIO

RANK	N	S	A	I
1	7.000	58.34	154.1	1.757
2	6.000	48.53	135.1	1.387
3	6.000	48.88	131.6	1.446
4	5.000	46.52	130.6	1.319
5	5.000	49.43	128.0	1.519
6	6.000	43.69	123.2	1.232
7	7.000	45.95	123.2	1.364
8	7.000	49.98	121.5	1.637
9	6.000	45.17	115.3	1.408
10	5.000	43.33	110.9	1.347
11	6.000	42.36	108.7	1.314
12	6.000	45.49	107.3	1.535
13	7.000	54.30	105.7	2.218
14	7.000	54.72	105.2	2.265
15	7.000	40.35	103.2	1.256
16	7.000	42.49	99.72	1.441
17	6.000	42.50	99.70	1.441
18	8.000	39.72	98.94	1.269
19	7.000	40.82	97.86	1.355
20	5.000	45.27	97.67	1.670
21	6.000	40.58	96.68	1.355
22	8.000	43.24	96.27	1.546
23	6.000	42.19	95.81	1.478
24	5.000	40.24	94.62	1.362
25	7.000	43.39	93.55	1.602

TABLE 4.7a

ANISOTROPIC CASE
$G_{(2,4,4,1,1,0,\pi/3)}$

SAMPLE SIZE 100000
PROCESSING RATE 5708/MIN

SAMPLE PERCENTILES

PROB(N = n)

n=	3	4	5	6	7
	.3543	.3899	.1872	.5527@-1	.1149@-1
n=	8	9	10	11	12
	.1650@-2	.1900@-3	.1000@-4	.0000	.0000

(0 POLYGONS WITH N > 12)

PROB(S < s)

s=	.1000	.2500	.5000	.7500	1.000
	.1030@-1	.2564@-1	.5227@-1	.7836@-1	.1050
s=	1.500	2.500	3.750	5.000	6.250
	.1576	.2582	.3769	.4805	.5714
s=	7.500	8.750	10.00	12.50	15.00
	.6486	.7144	.7696	.8525	.9060
s=	17.50	20.00	25.00	30.00	50.00
	.9406	.9636	.9866	.9953	.9999

(7 POLYGONS WITH S > 50)

PROB(A < a)

a=	.5000@-2	.1000@-1	.2500@-1	.5000@-1	.1000
	.4319@-1	.6074@-1	.9504@-1	.1338	.1868
a=	.2500	.5000	.7500	1.000	1.500
	.2841	.3844	.4510	.5047	.5815
a=	2.500	5.000	7.500	10.00	12.50
	.6814	.8125	.8758	.9123	.9356
a=	15.00	20.00	30.00	50.00	100.0
	.9514	.9710	.9881	.9973	.9998

(22 POLYGONS WITH A > 100)

TABLE 4.7b

ANISOTROPIC CASE
$G_{(2,4,4,1,1,0,\pi/3)}$

SAMPLE SIZE 100000
PROCESSING RATE 5708/MIN

SAMPLE MOMENTS

		N	S	A
1ST MOMENT	=	3.98548	6.78058	3.36630
(STD ERR)		.2996@-2	.1850@-1	.2124@-1
2ND MOMENT	=	16.7814	80.2053	56.4374
(STD ERR)		.2669@-1	.4577	1.239
3RD MOMENT	=	74.7903	1317.46	2209.25
(STD ERR)		.1913	13.45	146.7
4TH MOMENT	=	352.826	27381.3	156815.
(STD ERR)		1.313	480.1	.2220@5
5TH MOMENT	=	1759.49	683733.	.16480208
(STD ERR)		9.102	.1995@5	.3621@7
6TH MOMENT	=	9254.11	.19836108	.215716@10
(STD ERR)		65.05	.9199@6	.6087@9

KNOWN MOMENTS

		N	S	A
1TH MOMENT	=	4.00000	6.79264	3.39632
2TH MOMENT	=	16.9175	unknown	56.7235

TABLE 4.7c

ANISOTROPIC CASE
$G_{(2,4,4,1,1,0,\pi/3)}$

SAMPLE SIZE 100000
PROCESSING RATE 9700/MIN

THE 25 LARGEST POLYGONS (IN AREA)
I =ISOPERIMETRIC RATIO

RANK	N	S	A	I
1	7.000	54.63	178.4	1.331
2	7.000	54.21	175.7	1.331
3	5.000	57.40	174.8	1.500
4	7.000	49.75	163.8	1.202
5	5.000	51.21	160.0	1.304
6	5.000	54.94	143.2	1.677
7	9.000	51.48	142.3	1.482
8	7.000	45.37	140.4	1.167
9	7.000	51.50	139.4	1.514
10	6.000	44.86	129.8	1.234
11	7.000	44.09	124.8	1.239
12	6.000	41.83	116.1	1.199
13	7.000	42.93	113.9	1.288
14	6.000	44.81	113.7	1.406
15	8.000	41.50	111.7	1.227
16	6.000	49.77	110.8	1.780
17	7.000	45.09	110.1	1.469
18	5.000	45.48	106.1	1.551
19	7.000	42.53	105.1	1.370
20	7.000	43.22	101.8	1.460
21	4.000	41.52	101.5	1.351
22	7.000	44.36	101.4	1.545
23	5.000	46.87	99.82	1.751
24	6.000	41.51	97.77	1.403
25	5.000	45.86	96.44	1.735

4.5.3. Anisotropic Cases Induced by Q_ψ^D.

Tables 4.8a through 4.10c present the simulation results for the anisotropic cases induced by the three discrete uniform distributions in Q_ψ^D with atoms at 5, 10 and 20 points respectively. The functions $\lambda(\theta)$ for each of these distributions are obtained from (3.43).

As in the previous anisotropic simulations, the purpose here was exploratory so that sample sizes were also kept to 100,000. Simulation rates were still high, between 8275 and 6787 polygons per minute. Unfortunately, these cases were affected, though not so severely, by the same numerical problems discussed in the last subsection. Nonetheless, the general tendency for these cases to progressively approximate the isotropic case is readily apparent as expected. A deeper investigation into this convergence may well provide the key to obtaining the elusive analytic distributions of N, S, and A in the isotropic case.

TABLE 4.8a

ANISOTROPIC CASE
5 POINT DISCRETE UNIFORM

SAMPLE SIZE 100000
PROCESSING RATE 8275/MIN

SAMPLE PERCENTILES

PROB(N = n)

n=	3	4	5	6	7
	.3124	.4434	.1876	.4817@-1	.7590@-2

n=	8	9	10	11	12
	.8500@-3	.4000@-4	.0000	.0000	.0000

(0 POLYGONS WITH N > 12)

PROB(S < s)

s=	.1000	.2500	.5000	.7500	1.000
	.8990@-2	.2353@-1	.4897@-1	.7498@-1	.1005
s=	1.500	2.500	3.750	5.000	6.250
	.1526	.2553	.3772	.4873	.5820
s=	7.500	8.750	10.00	12.50	15.00
	.6638	.7316	.7873	.8697	.9219
s=	17.50	20.00	25.00	30.00	50.00
	.9540	.9735	.9907	.9971	1.000

(1 POLYGONS WITH S > 50)

PROB(A < a)

a=	.5000@-2	.1000@-1	.2500@-1	.5000@-1	.1000
	.3606@-1	.5258@-1	.8511@-1	.1214	.1735
a=	.2500	.5000	.7500	1.000	1.500
	.2714	.3731	.4436	.4976	.5781
a=	2.500	5.000	7.500	10.00	12.50
	.6824	.8155	.8805	.9168	.9406
a=	15.00	20.00	30.00	50.00	100.0
	.9561	.9740	.9891	.9976	.9999

(12 POLYGONS WITH A > 100)

TABLE 4.8b

ANISOTROPIC CASE
5 POINT DISCRETE UNIFORM

SAMPLE SIZE 100000
PROCESSING RATE 8275/MIN

SAMPLE MOMENTS

		N	S	A
1ST MOMENT	=	3.99792	6.50949	3.26471
(STD ERR)		.2785@-2	.1716@-1	.2010@-1
2ND MOMENT	=	16.7589	71.8088	51.0454
(STD ERR)		.2441@-1	.3951	.9927
3RD MOMENT	=	73.7311	1088.00	1774.38
(STD ERR)		.1710	10.64	88.86
4TH MOMENT	=	340.442	20764.2	101147.
(STD ERR)		1.136	340.1	.1090@5
5TH MOMENT	=	1648.46	474312.	.7997670 7
(STD ERR)		7.554	.1239@5	.1555@7
6TH MOMENT	=	8359.11	.12504@8	.7928090 9
(STD ERR)		51.30	.4945@6	.2373@9

KNOWN MOMENTS

		N	S	A
1TH MOMENT	=	4.00000	6.49839	3.24920
2TH MOMENT	=	17.1038	unknown	53.8825

TABLE 4.8c

ANISOTROPIC CASE
5 POINT DISCRETE UNIFORM

SAMPLE SIZE 100000
PROCESSING RATE 8275/MIN

THE 25 LARGEST POLYGONS (IN AREA)
I =ISOPERIMETRIC RATIO

RANK	N	S	A	I
1	9.000	48.44	165.2	1.131
2	7.000	51.31	145.6	1.439
3	7.000	44.56	129.9	1.216
4	6.000	43.36	118.6	1.261
5	6.000	43.22	116.4	1.277
6	7.000	44.55	110.5	1.429
7	6.000	41.82	110.1	1.264
8	5.000	45.12	106.3	1.525
9	7.000	43.45	105.0	1.431
10	6.000	41.57	104.8	1.312
11	6.000	44.59	103.3	1.531
12	6.000	39.67	103.2	1.213
13	5.000	39.05	97.75	1.241
14	7.000	39.52	96.85	1.284
15	5.000	39.08	94.47	1.287
16	8.000	38.32	91.76	1.274
17	6.000	38.55	91.24	1.296
18	7.000	37.01	91.18	1.195
19	6.000	38.57	90.52	1.308
20	8.000	36.84	89.98	1.200
21	6.000	41.81	88.16	1.578
22	7.000	37.10	88.04	1.244
23	8.000	36.72	87.88	1.221
24	5.000	39.16	87.24	1.399
25	5.000	38.03	86.30	1.333

TABLE 4.9a

ANISOTROPIC CASE
10 POINT DISCRETE UNIFORM

SAMPLE SIZE 100000
PROCESSING RATE 7142/MIN

SAMPLE PERCENTILES

PROB(N = n)

n=	3	4	5	6	7
	.3462	.3977	.1861	.5614@-1	.1194@-1
n=	8	9	10	11	12
	.1640@-2	.1900@-3	.3000@-4	.0000	.0000

(0 POLYGONS WITH N > 12)

PROB(S < s)

s=	.1000	.2500	.5000	.7500	1.000
	.1079@-1	.2701@-1	.5540@-1	.8201@-1	.1098
s=	1.500	2.500	3.750	5.000	6.250
	.1644	.2722	.3945	.5035	.5988
s=	7.500	8.750	10.00	12.50	15.00
	.6776	.7432	.7972	.8742	.9247
s=	17.50	20.00	25.00	30.00	50.00
	.9555	.9743	.9918	.9973	1.000

(0 POLYGONS WITH S > 50)

PROB(A < a)

a=	.5000@-2	.1000@-1	.2500@-1	.5000@-1	.1000
	.4214@-1	.5997@-1	.9462@-1	.1334	.1870
a=	.2500	.5000	.7500	1.000	1.500
	.2871	.3881	.4570	.5101	.5911
a=	2.500	5.000	7.500	10.00	12.50
	.6938	.8214	.8838	.9188	.9408
a=	15.00	20.00	30.00	50.00	100.0
	.9565	.9748	.9900	.9976	.9999

(15 POLYGONS WITH A > 100)

TABLE 4.9b

ANISOTROPIC CASE
10 POINT DISCRETE UNIFORM

SAMPLE SIZE 100000
PROCESSING RATE 7142/MIN

SAMPLE MOMENTS

		N	S	A
1ST MOMENT	=	3.99568	6.33138	3.16982
(STD ERR)		.2994@-2	.1704@-1	.1981@-1
2ND MOMENT	=	16.8619	69.1134	49.2739
(STD ERR)		.2675@-1	.3867	.9910
3RD MOMENT	=	75.2963	1040.33	1723.58
(STD ERR)		.1925	10.34	88.94
4TH MOMENT	=	355.871	19730.5	100635.
(STD ERR)		1.327	330.5	.1027@5
5TH MOMENT	=	1778.18	448133.	.81016307
(STD ERR)		9.265	.1206@5	.1330@7
6TH MOMENT	=	9374.35	.11772408	.79408109
(STD ERR)		66.95	.4808@6	.1830@9

KNOWN MOMENTS

		N	S	A
1TH MOMENT	=	4.00000	6.33538	3.16769
2TH MOMENT	=	16.9758	unknown	49.9284

TABLE 4.9c

ANISOTROPIC CASE
10 POINT DISCRETE UNIFORM

SAMPLE SIZE 100000
PROCESSING RATE 7142/MIN

THE 25 LARGEST POLYGONS (IN AREA)
I =ISOPERIMETRIC RATIO

RANK	N	S	A	I
1	8.000	48.24	154.7	1.197
2	7.000	49.50	134.3	1.452
3	6.000	46.57	134.1	1.288
4	6.000	44.75	130.1	1.225
5	7.000	44.15	124.2	1.248
6	7.000	46.05	119.9	1.408
7	7.000	44.04	115.5	1.336
8	8.000	41.41	114.0	1.197
9	7.000	43.80	111.6	1.368
10	8.000	41.42	108.0	1.265
11	10.00	38.58	105.2	1.127
12	8.000	47.09	104.9	1.683
13	5.000	46.93	104.4	1.679
14	7.000	42.27	102.3	1.390
15	6.000	40.33	100.1	1.293
16	8.000	38.55	98.64	1.199
17	7.000	44.38	96.85	1.618
18	7.000	41.14	95.65	1.408
19	7.000	40.26	94.78	1.361
20	8.000	42.48	94.61	1.518
21	6.000	38.97	94.11	1.284
22	6.000	37.62	92.39	1.219
23	6.000	37.19	91.78	1.199
24	7.000	39.40	91.50	1.350
25	6.000	42.91	90.23	1.624

TABLE 4.10a

ANISOTROPIC CASE
20 POINT DISCRETE UNIFORM

SAMPLE SIZE 100000
PROCESSING RATE 6787/MIN

SAMPLE PERCENTILES

PROB(N = n)

n=	3	4	5	6	7
	.3526	.3863	.1879	.5775E-1	.1316E-1
n=	8	9	10	11	12
	.1970E-2	.3100E-3	.0000	.0000	.0000

(0 POLYGONS WITH N > 12)

PROB(S < s)

s=	.1000	.2500	.5000	.7500	1.000
	.1155E-1	.2826E-1	.5704E-1	.8454E-1	.1127
s=	1.500	2.500	3.750	5.000	6.250
	.1684	.2769	.3988	.5070	.6025
s=	7.500	8.750	10.00	12.50	15.00
	.6804	.7451	.7989	.8755	.9253
s=	17.50	20.00	25.00	30.00	50.00
	.9565	.9752	.9917	.9974	1.000

(1 POLYGONS WITH S > 50)

PROB(A < a)

a=	.5000E-2	.1000E-1	.2500E-1	.5000E-1	.1000
	.4417E-1	.6309E-1	.9813E-1	.1368	.1918
a=	.2500	.5000	.7500	1.000	1.500
	.2926	.3931	.4617	.5145	.5941
a=	2.500	5.000	7.500	10.00	12.50
	.6960	.8228	.8840	.9200	.9428
a=	15.00	20.00	30.00	50.00	100.0
	.9577	.9755	.9900	.9978	.9998

(16 POLYGONS WITH A > 100)

TABLE 4.10b

ANISOTROPIC CASE
20 POINT DISCRETE UNIFORM

SAMPLE SIZE 100000
PROCESSING RATE 6787/MIN

SAMPLE MOMENTS

		N	S	A
1ST MOMENT	=	3.99967	6.28806	3.13505
(STD ERR)		.3048@-2	.1701@-1	.1962@-1
2ND MOMENT	=	16.9266	68.4676	48.3149
(STD ERR)		.2737@-1	.3854	1.005
3RD MOMENT	=	75.9519	1029.46	1696.74
(STD ERR)		.1982	10.36	102.4
4TH MOMENT	=	361.425	19540.3	103363.
(STD ERR)		1.377	336.6	.1457@5
5TH MOMENT	=	1821.48	445572.	.91913@7
(STD ERR)		9.669	.1262@5	.2397@7
6TH MOMENT	=	9698.74	.11801@8	.10515@10
(STD ERR)		69.95	.5214@6	.4198@9

KNOWN MOMENTS

		N	S	A
1TH MOMENT	=	4.00000	6.29614	3.14807
2TH MOMENT	=	16.9450	unknown	49.0064

TABLE 4.10c

ANISOTROPIC CASE
20 POINT DISCRETE UNIFORM

SAMPLE SIZE 100000
PROCESSING RATE 6787/MIN

THE 25 LARGEST POLYGONS (IN AREA)
I =ISOPERIMETRIC RATIO

RANK	N	S	A	I
1	8.000	52.38	184.9	1.181
2	8.000	44.19	137.1	1.134
3	6.000	46.45	134.8	1.274
4	7.000	49.20	132.6	1.452
5	8.000	45.14	128.3	1.264
6	8.000	44.46	115.6	1.361
7	6.000	41.96	115.2	1.216
8	7.000	48.73	114.9	1.645
9	9.000	42.17	112.3	1.260
10	8.000	46.31	109.9	1.553
11	6.000	45.88	107.8	1.554
12	7.000	47.26	107.2	1.658
13	6.000	39.88	104.2	1.214
14	6.000	44.18	103.2	1.505
15	6.000	42.06	101.5	1.387
16	7.000	40.03	101.3	1.258
17	7.000	39.28	94.88	1.294
18	5.000	41.28	94.79	1.431
19	6.000	44.09	92.69	1.669
20	6.000	36.90	92.49	1.172
21	6.000	39.63	91.40	1.367
22	6.000	38.79	90.37	1.325
23	6.000	38.71	90.06	1.324
24	7.000	37.73	89.77	1.262
25	5.000	40.13	88.71	1.444

APPENDIX

A.1. Characterizations of the Linear Poisson Process of (Constant) Intensity τ ($\ell pp\tau$).

A realization of a linear point process is a set of points on $\mathbb{R}$. It is well known that any of the following conditions is sufficient to completely characterize this process as an $\ell pp\tau$.

(A.1) (Counting Specification). Let N be a nonnegative integer-valued random Borel measure on $\mathbb{R}$. Then for k arbitrary disjoint Borel sets $A_1,\ldots,A_k$, $k = 1,2,\ldots$, the random variables $N(A_1),\ldots,N(A_k)$ have independent Poisson distributions with means $m(A_1),\ldots, m(A_k)$, where m is Lebesgue measure. (Note that it is sufficient to specify this property for intervals $A_1,\ldots,A_k$).

(A.2) (Interval Specification). If 0 is an arbitrary time origin and the process points are labelled according to the definition $\ldots \leq T_{-2} \leq T_{-1} \leq T_0 \leq 0 \leq T_1 \leq T_2 \leq \ldots$, then the intervals $T_{-1}-T_{-2}$, T_0-T_{-1}, $-T_0$, T_1, $T_2-T_1,\ldots$ are a sequence of iid exponentially distributed random variables with parameter τ.

(A.3) (Local Intensity Specification). As in (A.1) let N be a nonnegative integer-valued random Borel measure on $\mathbb{R}$. Let $\mathcal{H}(t)$ denote the history of the processes at time t. Then as $\delta \to 0^+$,

$$P\{N(t,t+\delta) = 1 | \mathcal{H}(t)\} = \tau\delta + O(\delta)$$

and

$$P\{N(t,t+\delta) > 1 | \mathcal{H}(t)\} = o(\delta) \ .$$

(Note that the second condition here virtually excludes the possibility of multiple occurrences.)

There are several other known ways of characterizing a $\ell pp\tau$. For a list of these, together with references, see Cox and Isham (1980).

A.2. An Integral Formula for $E[A^4]$

We here derive an integral formula for the fourth moment of A in isotropic $\mathcal{P}^*$. We proceed by exact analogy with the derivation of $E[A^2]$ in Coudsmit (1945) and the generalization for deriving $E[A^3]$ in Solomon (1978). The basic idea is to derive two expressions for the probability that four random points in a large area D lie inside the same polygon. We shall denote this probability by P_4. The two expressions are then equated, the area $D \to \infty$, and our formula is obtained.

The first expression for P_4 is obtained as follows. Let $h(\sigma)$ be the probability density of A. Let M be the number of polygons in D. Then the probability that a random point in D lies inside a polygon of area between σ and $\sigma + d\sigma$ is approximately

$$\sigma M h(\sigma) d\sigma / D \ .$$

The probability that three more random points lie inside this same polygon is $(\sigma/D)^3$. Thus we obtain

$$P_4 = \frac{M}{D^4} \int_0^\infty \sigma^4 h(\sigma) d\sigma = \frac{M}{D^4} E[A^4] \ . \tag{A.4}$$

The second expression is obtained by averaging over all positions of four random points, the probability that no line in $\mathcal{L}$ passes through the convex hull, denoted by C, of these four points. This is equivalent to their lying in the same polygon.

We denote the four points by x_1, x_2, x_3, and x_4. Without loss of generality, we orient the horizontal axis so that x_1 is at the

origin and x_2 lies along the axis in the positive direction. Let $r_i = |x_{i+1} - x_1|$, $i = 1,2,3$. Let θ_1 be the angle between r_1 and r_2 and θ_2 the angle between r_1 and r_3. See Figure A.1.

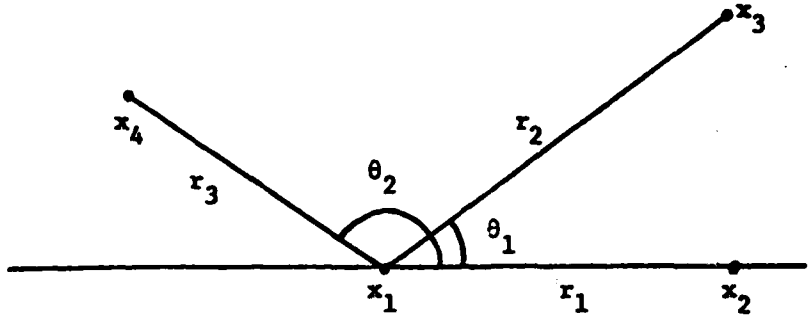

Figure A.1

We write $\underset{\sim}{r} = (r_1, r_2, r_3, \theta_1, \theta_2)$ and let $p(\underset{\sim}{r})$ be the perimeter of C. We have by an easy generalization of Theorem 1.2.4 that the probability that no line of $\mathcal{L}$ crosses C is

$$e^{-\tau p(\underset{\sim}{r})/\pi} . \tag{A.5}$$

Notice that when the line segments joining the four points x_1, x_2, x_3, x_4 form a reentrant quadrilateral, C is a triangle. Otherwise, C is a convex quadrilateral.

In terms of differentials, the probability that a particular orientation lies between $\underset{\sim}{r}$ and $\underset{\sim}{r} + d\underset{\sim}{r}$ is

$$2\pi\, r_1\, r_2\, r_3\, d\underset{\sim}{r}/D^3 ,$$

the ratio of the differential volume element to the total volume. Combining this with (A.5) yields

(A.6) $$P_4 = \mu(E)/D^3 + o(1)$$

where

(A.7) $$\mu(E) = 2\pi \iiint_E e^{-\tau p(\underset{\sim}{r})/\pi} r_1 r_2 r_3 \, d\underset{\sim}{r}$$

and

$$E = \{\underset{\sim}{r}: 0 \leq r_i < \infty, \ i = 1,2,3 \ \text{ and } \ 0 \leq \theta_j \leq 2\pi, \ j = 1,2\}$$

is the set of all positions of the four points in the plane. The term $o(1) \to 0$ as $D \to \infty$ in (A.6) accounts for the part of E not included in D. That this is the correct order term follows by noting that $p(\underset{\sim}{r}) > r_i$, $i = 1,2,3$.

Equating (A.4) and (A.6) we have as $D \to \infty$

(A.8) $$E[A^4] = \lim_{D\to\infty} \frac{D}{M} \mu(E)$$

$$= \frac{\pi}{\tau^2} \mu(E)$$

since $\lim_{D\to\infty} D/M = E[A] = \pi/\tau^2$. (See Solomon (1978)).

We now proceed to reduce E by symmetry arguments. First

$$\mu(E_1) = \frac{1}{2} \mu(E)$$

where

$$E_1 = E \cap \{\underset{\sim}{r}: 0 \leq \theta_1 \leq \theta_2 \leq 2\pi\} .$$

Next observe that the integration in (A.7) is the same for regions of E_1 where x_2, x_3, x_4 all lie in the same half-plane. Hence,

$$\mu(E_2) = \mu(E_3) = \mu(E_4)$$

where

$$E_2 = E_1 \cap \{\underset{\sim}{r}: 0 \leq \theta_1 < \theta_2 \leq \pi\}$$

$$E_3 = E_1 \cap \{\underset{\sim}{r}: \pi \leq \theta_1 < \theta_2 \leq 2\pi\}$$

$$E_4 = E_1 \cap \{\underset{\sim}{r}: 0 \leq \theta_1+\pi < \theta_2 \leq 2\pi\} .$$

Finally let

$$E_5 = E_1 \cap \{\underset{\sim}{r}: 0 < \theta_1 < \pi < \theta_2 < \theta_1+\pi \leq 2\pi\}$$

so that

$$E_1 = E_2 \cup E_3 \cup E_4 \cup E_5 .$$

Combining the above we have

(A.9) $$\mu(E) = 6\mu(E_2) + 2\mu(E_5) .$$

We now proceed to express $p(\underset{\sim}{r})$ explicitly on the sets E_2 and E_5. Define

(A.10) $$h(\underset{\sim}{r}) = \frac{r_1}{\cos\theta_1 + \sin\theta_1 \left(\frac{r_1 - r_3\cos\theta_2}{\sin\theta_2}\right)} .$$

$h(\underset{\sim}{r})$ is the distance along the line coincident with r_2, from x_1 to the line connecting x_2 and x_4.

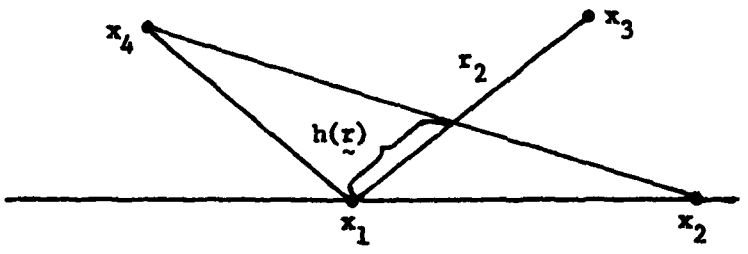

Let

$$E_6 = E_2 \cap \{\underset{\sim}{r}: r_2 \leq h(\underset{\sim}{r})\}$$

$$E_7 = E_2 \cap \{\underset{\sim}{r}: r_2 > h(\underset{\sim}{r})\} .$$

Notice that $\underset{\sim}{r} \in E_6$ implies C is a triangle and $\underset{\sim}{r} \in E_7$ implies C is a quadrilateral.

For notational convenience, write the distance $|x_{i+1} - x_{j+1}|$ as

$$d(r_i,r_j) = (r_i^2 + r_j^2 - 2r_i r_j \cos \alpha_{ij})^{1/2}$$

$$\alpha_{12} = \theta_1, \ \alpha_{13} = \theta_2, \ \alpha_{23} = \theta_2 - \theta_1 .$$

Then

$$\text{(A.11)} \qquad p(\underset{\sim}{r}) = \begin{cases} r_1 + r_3 + d(r_1,r_3) & \text{on } \underset{\sim}{r} \in E_6 \\ r_1 + r_3 + d(r_1,r_2) + d(r_2,r_3) & \text{on } \underset{\sim}{r} \in E_7 . \end{cases}$$

Also since $r \in E_5$ implies C is a triangle we have

$$\text{(A.12)} \qquad p(\underset{\sim}{r}) = d(r_1,r_2) + d(r_2,r_3) + d(r_1,r_3) \quad \text{on } \underset{\sim}{r} \in E_5 .$$

Combining this reduction with (A.8) and (A.9) we obtain

$$\text{(A.13)} \qquad E[A^4] = \frac{\pi}{\tau^2} [6\mu(E_6) + 6\mu(E_7) + 2\mu(E_5)]$$

where

$$\mu(E_i) = 2\pi \iiint_{E_i} e^{-\tau p(\underset{\sim}{r})/\pi} \, r_1 \, r_2 \, r_3 \, d\underset{\sim}{r}$$

and

$$E_6 = \{\underset{\sim}{r}: 0 \le r_1 < \infty,\ 0 \le r_2 \le h(\underset{\sim}{r}),\ 0 \le r_3 < \infty,$$
$$0 \le \theta_1 < \theta_2 \le \pi\}$$

$$E_7 = \{\underset{\sim}{r}: 0 \le r_1 < \infty,\ h(\underset{\sim}{r}) < r_2 < \infty,\ 0 \le r_3 < \infty,$$
$$0 \le \theta_1 < \theta_2 \le \pi\}$$

$$E_5 = \{\underset{\sim}{r}: 0 \le r_i < \infty,\ i = 1,2,3 \text{ and}$$
$$0 < \theta_1 < \pi < \theta_2 < \theta_1 + \pi \le 2\pi\}\ .$$

Writing out (A.13) more explicitly we have the integral formula

$$\text{(A.14)}\quad E[A^4] = \frac{4\pi^2}{\tau^2}\left[\left\{3\int_0^{\pi}\int_0^{\theta_2}\int_0^{\infty}\int_0^{\infty}\left(\int_0^{h(\underset{\sim}{r})} e^{-\frac{\tau}{\pi}(r_1+r_3+d(r_1,r_3))} r_2 dr_2 \right.\right.\right.$$
$$\left.\left.\left. + \int_{h(\underset{\sim}{r})}^{\infty} e^{-\frac{\tau}{\pi}(r_1+r_3+d(r_1,r_2)+d(r_2,r_3))} r_2 dr_2\right) r_1 r_3 dr_1 dr_3 d\theta_1 d\theta_2\right\}$$
$$+\left\{\int_{\pi}^{2\pi}\int_{\theta_2-\pi}^{\pi}\int_0^{\infty}\int_0^{\infty}\int_0^{\infty} e^{-\frac{\tau}{\pi}(d(r_1,r_2)+d(r_2,r_3)+d(r_1,r_3))}\right.$$
$$\left.\left. r_1 r_2 r_3 dr_1 dr_2 dr_3 d\theta_1 d\theta_2\right\}\right]$$

where $h(\underset{\sim}{r})$ is defined in (A.10).

A.3. A Theorem on the Richness of $\mathcal{Q}^C$.

Theorem. $\mathcal{Q}^C$ defined in (3.31) is dense in the class $\mathcal{D}$ of continuous probability densities on $[0,\pi]$.

Proof. Let $f \in \mathcal{D}$ and pick $\varepsilon > 0$. f is uniformly continuous so $\exists\ \delta > 0$ s:

$$|f(\theta_1) - f(\theta_2)| < \frac{\varepsilon}{4} \quad \text{if} \quad |\theta_1 - \theta_2| < 2\delta . \tag{A.15}$$

Let $M = \max f(\theta)$. Then $\exists\ m_0$ s: $\forall\ \theta$,

$$\int_{\theta-\delta}^{\theta+\delta} |\sin^{m_0}(\theta-\omega)| \frac{d\omega}{K_{m_0}} \geq 1 - \frac{\varepsilon}{4M} \tag{A.16}$$

(see (3.33) for definition of K_m).

Combining (A.15) and (A.16), we have uniformly in θ

$$\left| \int_0^{\pi} f(\omega) |\sin^{m_0}(\theta-\omega)| \frac{d\omega}{K_{m_0}} - f(\theta) \right| \tag{A.17}$$

$$\leq \int_0^{\pi} |f(\omega)-f(\theta)|\,|\sin^{m_0}(\theta-\omega)|\, \frac{d\omega}{K_{m_0}}$$

$$< \frac{\varepsilon}{4}\left(1 - \frac{\varepsilon}{4M}\right) + M \cdot \frac{\varepsilon}{4M} < \frac{\varepsilon}{2} .$$

Define

$$h_n(\theta) = \frac{\pi}{K_{m_0} n} \sum_{i=1}^{n} f\left(\frac{i\pi}{n}\right) \left|\sin^{m_0}\left(\theta - \frac{i\pi}{n}\right)\right|$$

and

$$g_n(\theta) = \frac{1}{K_{m_0} \sum_{j=1}^{n} f\left(\frac{i\pi}{n}\right)} \cdot \sum_{i=1}^{n} f\left(\frac{i\pi}{n}\right) \left|\sin^{m_0}\left(\theta - \frac{i\pi}{n}\right)\right| .$$

We can choose N large enough so that $\forall\ \theta$

$$|h_N(\theta) - \int_0^{\pi} f(\omega)\,|\sin^{m_0}(\theta-\omega)|\,\frac{d\omega}{K_{m_0}}| < \frac{\varepsilon}{4} \tag{A.18}$$

by direct Riemann approximation, and

$$|g_N(\theta) - h_N(\theta)| < \frac{\varepsilon}{4} \tag{A.19}$$

because

$$\frac{\pi}{N}\sum_{j=1}^{N} f(\tfrac{j\pi}{N}) \to \int_0^{\pi} f(\theta)\,d\theta = 1\ .$$

Combining (A.17), (A.18), and (A.19) we have $\forall\ \theta$

$$|g_N(\theta) - f(\theta)| < \varepsilon\ .$$

But

$$g_N(\theta) = G_{(n,m,\alpha,\beta)}(\theta) \in C_{\mathring{}}^{C}\ ,$$

where $n=N$ and for $i = 1,\ldots,N$, $m_i = m_0$, $\alpha_i = \frac{i\pi}{N}$, and

$$\beta_i = \frac{f(\frac{i\pi}{N})}{\sum_{j=1}^{N} f(\frac{j\pi}{N})}\ . \qquad \|$$

A.4. Splitting Probabilities and the Distribution of N.

Consider a random secant through an N-sided polygon in isotropic ρ^*. That is, let the secant coincide with a line whose coordinates (P,θ) are distributed proportionally to $dpd\theta$ over the set of lines hitting the polygon. This secant 'splits' the polygon into left and right polygons which we define as lying to the left and right respectively of the lower intersection of the secant with the polygon, see Figure A.2.

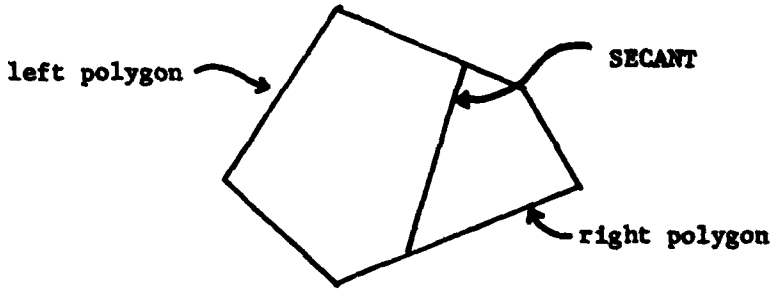

Figure A.2

Define the left splitting probability p^*_{ij}, where $i = 3,4,\ldots,$ and $j = 3,\ldots,i+1,$ to be the probablity that a random secant through a random i-sided polygon in ρ^* yields a j-sided left polygon.

The following system of equations expresses the interrelation between the distribution of N and the splitting probabilities. Knowledge of either set of probabilities should enable us to solve this system for the other.

$$(A.20) \qquad P\{N=m\} = \sum_{i=m-1}^{\infty} (i-2)\, P\{N=i\} p^*_{im}, \quad m = 3,4,\ldots .$$

We shall outline a derivation of (A.20) which is based on the invariance of the distribution of N under changes in the intensity τ of the Poisson line process. Consider a random secant through the portion of ρ^* contained in a large disc of radius q. As in the proof of Theorem 1.2.4 it is easily shown that the probability that this secant hits a polygon with perimeter s is proportional to s. Define $p_{i,s}^{H_q}$ to be the probability density that this secant hits an i-sided polygon with perimeter s. Then,

$$p_{i,s}^{H_q} \propto s \, dP_q\{S = s, N = i\}$$

where $P_q\{S = s, N = i\}$ is the joint density of S and N in the disc. Now let $q \to \infty$ so that the random secant will correspond to a new line resulting from an infintesimal increase in the intensity τ of the Poisson line process. Then $p_{i,s}^{H_q} \to p_{i,s}^{H}$, the probability density of i-sided polygons with perimeter s along the new line. Furthermore, since $P_q\{S = s, N = i\} \to P\{S = s, N = i\}$ the ergodic density, we have

$$p_{i,s}^{H} \propto s \, dP\{S = s, N = i\} \quad . \tag{A.21}$$

Define p_i^H to be the probaiblity density of i-sided polygons along the new line. Integrating (A.21) we obtain

$$\begin{aligned} p_i^H &\propto \int s \, dP\{S = s, N = i\} \\ &\propto \int s \, dP\{S = s | N = i\} \cdot P\{N = i\} \\ &\propto E\{S | N = i\} \cdot P\{N = i\} \quad . \end{aligned}$$

But from Section 3.5 we have $E\{S|N=i\} \propto (i-2)$ and $E[N] = 4$, so that

$$p_i^H = \frac{1}{2}(i-2) \cdot P\{N=i\} \quad .$$

Finally, this new line creates two polygons for every one it hits. However, because of the invariance of the distribution of N under the addition of one more line, the distribution of N of the new polygons must be this same distribution. By the symmetry between left and right new polygons, we have for $m = 3,4,\ldots$

$$P\{N=m\} = 2 \cdot \sum_{i=m-1}^{\infty} p_i^H p_{im}^*$$

$$= \sum_{i=m-1}^{\infty} (i-2)\, P\{N=i\} p_{im}^* \quad .$$

We remark that a little more simplification of (A.20) is possible because $p_{im}^* = p_{i(i+4-m)}^*$ by symmetry.

FOOTNOTES

[1] The agreement of some of his results with those of Goudsmit (when suitably normalized) suggests that Goudsmit had in mind this very model.

[2] The in-circle of a convex polygon is the largest circle it contains. While it may not be unique, its diameter is. We shall not investigate this ch racteristic further as it seems to be less important than N, S, or A.

[3] The particular paper, Miles (1973), came to the attention of the author after the bulk of the present work had been carried out. His stochastic constructions seem not to be of the sequential nature of the construction developed here, although both processes begin with a similar step. Apparently, his constructions are not very efficient for simulation studies as he chose a different method in his later Monte Carlo study with Crain. Furthermore, as he does not elaborate on the details of his construction, it is hard to see the mathematical potential, although he does allude to some recursive integral equations for the distributions of polygon characteristics. Finally, his constructions are given for the isotropic case whereas the sequential construction here is developed in the general translation invariant context. The essential overlap of Miles' contribution with the present paper is that both constructions yield sets of polygons equivalent to an independent and identically distributed sample of polygons from a Poisson field of lines.

[4] Some researchers in the line processes consider directed lines and use this parametrization with $\theta \in [0, 2\pi)$. We will be concerned only with undirected lines.

[5] C is endowed with the ordinary Euclidean topology.

[6] Some researchers (Davidson (1974)) consider the more general doubly stochastic Poisson line process. The equivalent point process on C then has the same distributional form as (1.5) with m replaced by a random Borel measure Λ. We shall not consider this generalization here.

[7] It actually takes a little doing to establish this from (1.5). A possible derivation establishes a characterization like (A.3) for multivariate Poisson processes from which a joint conditional density can be derived. we do not carry out the details as this seems to be a well known property.

[8] We use the term density throughout this work to refer to the differential element of the measure referred to. For example, if μ is a measure, then we refer to $d\mu$ as the density where $\mu(A) = \int_A d\mu$. Note that contrary to common usage, we include the differential element of the carrier measure.

[9] For isotropic μ^* the curling process can be modified to select a sample from a population equivalent up to translation and rotation.

[10] We condition on the open interval $(\alpha_{n-1}, \theta_{n-1})$ here. When the distribution G of θ is continuous, it trivially does not matter. However, this restriction is essential if G has an

atom at either α_{n-1} or θ_{n-1}. Any such value would violate the property that the Poisson point process on C has no multiple points (a property similar to (A.3)).

[11] See formula (5.19) in Miles (1973). Miles uses a different parametrization of the angles, but his side lengths L_i are the same as our Z_i.

[12] For example, a natural candidate would be the circular normal distribution where the density is proportional to $\exp\{-K \cos 2\theta\}$, see Mardia (1972). The reader can verify that a closed form expression for F in (3.29) is unobtainable.

[13] The Monte Carlo study of Crain and Miles (1976) exploits information from one of these aggregates, the perimeter weighted + polygons, (see also footnote [15]).

[14] Result communicated to H. Solomon in unpublished memo. See Solomon (1978), p. 54.

[15] Actually Crain and Miles consider two types of polygons, *polygons which are the same as ours, and +polygons which are the unions of pairs of adjacent polygons. They simulated 100,495 *polygons and 95,485 +polygons in 45 and 21 sample discs, respectively. The distributions of +polygon characteristics correspond to a perimeter weighting of those *polygons. Table 4.2 presents some estimates of the distribution of N based on +polygons, (see also footnote [17]). In particular, extreme values of N, S, and A are more likely in the + polygon population so that more precise estimates of the tails are available.

[16] The computer operators at the IMSSS facility, Stanford, Ca., estimate that our machine, the PDP10/KI is about twice as fast as the IBM 360/50 used by Crain and Miles. They added however that the comparison is difficult.

[17] We present in this table the different estimates that Crain and Miles obtain for the distribution of N. *STD and +STD estimates are ordinary sample averages using *polygons and +polygons respectively, (see footnote [15]). *WTD and +WTD are the corresponding weighted estimates compensating for the edge effects. QRF and CRF refer to quadratic and cubic ratio fits obtained by fitting polynomial expressions for ratios of probabilities to the data and known values. Crain and Miles present histograms rather than percentile estimates for S and A, together with various types of moment estimates.

[18] We programmed the Monte Carlo simulations in the programming language SAIL (Stanford Artificial Intelligence Laboratory). This language includes as a standard subroutine a pseudo-random number generator called RAN.

[19] Private communication to H. Solomon.

[20] Our programming language SAIL is basically an algorithmically oriented language for programming ease. The variables used hold at most eight significant digits rendering it somewhat inaccurate for sophisticated numerical work. Apparently a new extended precision version of SAIL will soon be available. Alternatively, the extended precision capability of FORTRAN makes it an ideal language for this type of simulation. The author plans to carry

out more extensive simulations of these sensitive anisotropic cases with a more numerically precise programming language in the future.

REFERENCES

Baddeley, A. (1977), "A Fourth Note on Recent Research in Geometrical Probability," Adv. Appl. Prob. 9, 824-860.

Butler, J. W. (1954), "Machine Sampling from Given Probability Distributions," in Meyer, H. A. (ed.), Symposium on Monte Carlo Methods. Wiley, N.Y.

Cowan, R. (1978), "The Use of Ergodic Theorems in Random Geometry," Suppl. Adv. Appl. Prob. 10, 47-57.

Cox, D. R. and Isham, V. (1980), Point Processes, Chapman and Hall, London.

Crain, I. K. and Miles, R. E. (1976), "Monte Carlo Estimates of the Distributions of the Random Polygons Determined by Random Lines in a Plane," J. Stat. Comp. 4, 293-325.

Crofton, M. W. (1885), "Probability," Encyclopedia Britannica, 9th ed., Vol. 19, 768-788.

Davidson, R. (1974), "Constructing of Line Processes: Second Order Properties," in Harding and Kendall (eds.), Stochastic Geometry, Wiley, N.Y., 55-75.

Dwight, H. B. (1961), Tables of Integrals and Other Mathematical Data, Macmillan, N.Y.

Goudsmit, S. A. (1945), "Random Distribution of Lines in a Plane," Rev. Mod. Phys. 17, 321-322.

Hammersley, J. M. and Handscomb, D. C. (1964), Monte Carlo Methods, Metheun, London.

Harding, E. F. and Kendall, D. G. (1974), Stochastic Geometry, Wiley, N.Y.

Little, D. V. (1974), "A Third Note on Recent Research in Geometrical Probability," Adv. Appl. Prob. 6, 103-130.

Mardia, K. V. (1972), Statistics of Directional Data, Academic Press, N.Y.

Miles, R. E. (1964), "Random Polygons Determined by Random Lines in a Plane," Proc. Nat. Acad. Sci. (USA), Part I 52, 901-907; Part II 52, 1157-1160.

Miles, R. E. (1971), "Poisson Flats in Euclidean Spaces. II," Adv. Appl. Prob. 3, 1-43.

Miles, R. E. (1974), "On the Elimination of Edge Effects in Planar Sampling," in Harding and Kendall (eds.), Stochastic Geometry, Wiley, N.Y., 227-247.

Miles, R. E. (1973), "The Various Aggregates of Random Polygons Determined by Random Lines in a Plane," Adv. Math. 10, 256-290.

Moran, P. A. P. (1966), "A Note on Recent Research in Geometrical Probability," J. Appl. Prob. 3, 453-463.

Moran, P. A. P. (1969), "A Second Note on Recent Research in Geometrical Probability," Adv. Appl. Prob. 1, 73-89.

Santalo, L. A. (1953), Introduction to Integral Geometry, Hermann, Paris (Act. Sci. Indust. No. 1198).

Santalo, L. A. (1976), "Integral Geometry and Geometric Probability," Encyclopedia of Mathematics and Its Applications, Vol. 1, Addison-Wesley, MA.

Solomon, H. and Wang, P. (1972), "Nonhomogeneous Poisson Fields of Random Lines with Applications to Traffic Flow," Proc. Sixth Berkeley Symp. Math. Statist. Prob. 3, 383-400.

Solomon, H. (1978), Geometrical Probability, SIAM Publications (CBMS-NSF 28), PA.

Solomon, H. and Stephens, M. A. (1980), "Approximations to Densities in Geometrical Probabiligy," J. Appl. Prob. 17, 145-153.

Snyder, D. L. (1975), Random Point Processes, Wiley, N.Y.

UNCLASSIFIED

SECURITY CLASSIFICATION OF THIS PAGE (When Data Entered)

REPORT DOCUMENTATION PAGE		READ INSTRUCTIONS BEFORE COMPLETING FORM
1. REPORT NUMBER: 320	2. GOVT ACCESSION NO.: AD-A119410	3. RECIPIENT'S CATALOG NUMBER:
4. TITLE (and Subtitle): SEQUENTIAL STOCHASTIC CONSTRUCTION OF RANDOM POLYGONS		5. TYPE OF REPORT & PERIOD COVERED: TECHNICAL REPORT
		6. PERFORMING ORG. REPORT NUMBER:
7. AUTHOR(s): Edward Ian George		8. CONTRACT OR GRANT NUMBER(s): N00014-76-C-0475
9. PERFORMING ORGANIZATION NAME AND ADDRESS: Department of Statistics Stanford University Stanford, CA 94305		10. PROGRAM ELEMENT, PROJECT, TASK AREA & WORK UNIT NUMBERS: NR-042-267
11. CONTROLLING OFFICE NAME AND ADDRESS: Office Of Naval Research Statistics & Probability Program Code 411SP Arlington, VA 22217		12. REPORT DATE: June 10, 1982 13. NUMBER OF PAGES: 134
14. MONITORING AGENCY NAME & ADDRESS(if different from Controlling Office)		15. SECURITY CLASS. (of this report): UNCLASSIFIED 15a. DECLASSIFICATION/DOWNGRADING SCHEDULE

16. DISTRIBUTION STATEMENT (of this Report)

APPROVED FOR PUBLIC RELEASE: DISTRIBUTION UNLIMITED.

17. DISTRIBUTION STATEMENT (of the abstract entered in Block 20, if different from Report)

18. SUPPLEMENTARY NOTES

19. KEY WORDS (Continue on reverse side if necessary and identify by block number)

Poisson fields of lines; distributions of sides, parameter and area of random polygons; isotropic and anisotropic cases.

20. ABSTRACT (Continue on reverse side if necessary and identify by block number)

PLEASE SEE REVERSE SIDE.

DD FORM 1 JAN 73 1473 EDITION OF 1 NOV 65 IS OBSOLETE
S/N 0102-LF-014-6601

UNCLASSIFIED

SECURITY CLASSIFICATION OF THIS PAGE (When Data Entered)

#320

Homogeneous Poisson fields of lines divide the plane into non-overlapping convex polygons. Of interest to researchers in geometrical probability have been the distributions of characteristics of the polygons induced by the distributions of the lines, especially N, the number of sides, S, the perimeter, and A, the area. A sequential stochastic process is developed from which an independent and identically distributed sample of polygons can be extracted with a stopping time. It is shown that the distribution of polygons so obtained is identical to the distribution of polygons in the Poisson field. The stochastic process is developed in full generality and can be applied to anisotropic cases as well as the case of most interest, the isotropic case. Useful families of anisotropic distributions for this problem are defined.

The sequential stochastic process is used to derive general analytical expressions for polygon distributions for the investigation of the unknown distributions of N, S and A. Methods are also developed which provide the basis for very fast computer simulation of the process. A Monte Carlo study of the distributions of N, S, and A in various cases is presented. In particular, a sample of 2,500,000 polygons in the isotropic case provides the most precise results to date.

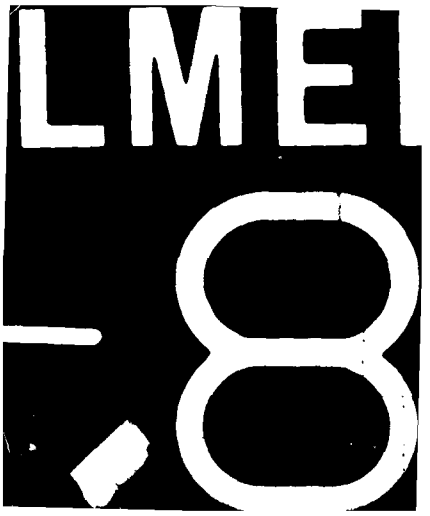
LME
.8